**Calhoun: The NPS Institutional Archive**

**DSpace Repository**

Theses and Dissertations                                   1. Thesis and Dissertation Collection, all items

1973

# Marine environment effects on fatigue crack propagation in GRP laminates for hull construction.

Demchik, Robert Paul.

Massachusetts Institute of Technology

http://hdl.handle.net/10945/16692

# MARINE ENVIRONMENT EFFECTS ON FATIGUE CRACK PROPAGATION IN GRP LAMINATES FOR HULL CONSTRUCTION

Robert Paul Demchik

MARINE ENVIRONMENT EFFECTS ON FATIGUE CRACK PROPAGATION

IN GRP LAMINATES FOR HULL CONSTRUCTION

BY

ROBERT PAUL DEMCHIK

LIEUTENANT COMMANDER, UNITED STATES NAVY

B.S., United States Naval Academy

1964

SUBMITTED IN PARTIAL FULFILLMENT

OF THE REQUIREMENTS FOR THE DEGREE OF

OCEAN ENGINEER

AND THE DEGREE OF

MASTER OF SCIENCE IN

NAVAL ARCHITECTURE AND MARINE ENGINEERING

at the

Massachusetts Institute of Technology

May, 1973

# MARINE ENVIRONMENT EFFECTS ON FATIGUE CRACK PROPAGATION

## IN GRP LAMINATES FOR HULL CONSTRUCTION

BY

ROBERT PAUL DEMCHIK

## ABSTRACT

The effects of a salt water environment on the fatigue
properties of a particular GRP laminate construction ,
suitable for hull construction, are examined experimentally.
The experimental S-N curves for both an air and a salt
water environment are given and comparison of the two
curves shows a general, but moderate, decrease in the
fatigue life of the material in a salt water environment.
A recently developed theory for fatigue crack growth
in composite materials is used as the basis for compari-
son of experimental data obtained for the relationship
between fatigue crack growth rate and stress intensity
factor.  The theory is confirmed for the specific material
used in this study when a linear approximation to the S-N
curves is made.  Further, the mechanism of fatigue crack
growth is confirmed as one of ligament advance.
Additional experimental work to refine the theory is
recommended.

THESIS SUPERVISOR:  FREDERICK J. MCGARRY

TITLE:  PROFESSOR, DEPARTMENT OF CIVIL ENGINEERING

## ACKNOWLEDGMENTS

I wish to express my sincere appreciation to Professor Frederick J. McGarry, Department of Civil Engineering, Massachusetts Institute of Technology, for his advice, guidance and encouragement throughout the duration of this work. I am also very much indebted to Doctor John Mandell of the same department whose invaluable knowledge and experience were instrumental in assisting with the successful completion of the study.

The assistance and advice of Mr. Arthur Rudolph were of great value in the manufacture of the salt water containment system and in the machining of the specimens. Considerable help in the conduct of some of the tests and in the development of the dogbone specimen shape was contributed by graduate student Reiichiro Kashihara and is very much appreciated.

Finally, I wish to thank my wife Nancy whose tolerance and understanding were pushed to the very limit during the final hectic days of the work.

# TABLE OF CONTENTS

# LIST OF SYMBOLS

$a$ = Notch/Crack length measured from centerline of applied load - inches

$B$ = Specimen thickness - inches

$C$ = Specimen compliance - in/lb

$d$ = Ligament size - inches

$\frac{da}{dN}$ = Fatigue crack propagation rate - in/cycle

$E$ = Young's Modulus - ksi

$G$ = Strain energy release rate - lb/in

$H$ = Index card specimen half-width - inches

$K_I$ = Opening mode stress intensity factor - ksi-in$^{\frac{1}{2}}$

$K_Q$ = Candidate critical stress intensity factor - ksi-in$^{\frac{1}{2}}$

$N$ = Number of cycles under fatigue loading

$P_{max}$ = Maximum load in a fatigue load cycle - lb

$P_{mean}$ = Mean load in a fatigue load cycle - lb

$P_{min}$ = Minimum load in a fatigue load cycle - lb

$P_{range}$ = Load range of a fatigue load cycle - lb

$s$ = Slope of linear S-N curve - psi/decade of cyc.

$\Delta l$ = Deflection between loading points on Instron Universal Testing Machine - inches

$\sigma$ = General stress value along S-N curve - ksi

$\sigma_1$ = Local stress at crack tip - ksi

$\sigma_f$ = Ultimate tensile strength - ksi

# I.  INTRODUCTION

The development of glass fiber-reinforced plastics
has advanced to a point where these materials are now con-
sidered serious competitors for the more standard structural
materials such as wood, metals and concrete for many app-
lications.  The recent construction of a 153-foot minehunt-
er, HMS Wilton, by the British (1) is witness to the feasi-
bility of building larger, sea-going vessels of reinforced
plastics.  What problems may develop after a significant
service life remain to be seen.  Meanwhile, investigations
must continue that will add to the store of knowledge about
the properties of these materials.

A substantial amount of investigation has been conducted
into the fracture toughness properties of various glass-
plastic composites.  Emphasis in many studies has been on
determining whether the principles of fracture mechanics as
developed for homogeneous materials, and widely applied to
metals, might be applicable to composites.  In general, it
seems to have been established that such is, indeed, the
case with some modifications (2).

One aspect of the fracture of glass-reinforced composites
that has received little attention to date is the fatigue
life.  Fatigue fracture is defined as the failure of a mat-
erial under repeated loading.  The higher the cyclical
stress, the lower will be the number of cycles endured to
failure.  The fatigue characteristics of a material are

commonly displayed in the form of a Wohler, or S-N, curve which gives the number of cycles to failure at a given nominal stress. Ferrous metals exhibit a fatigue limit defined simply as a stress below which the fatigue life is considered infinite (3).

Fatigue properties must be adequately defined in order to insure proper and safe design of a structure - particularly a structure that can be expected to see repeated loadings during its lifetime. Structural components in the vicinity of machinery foundations or in other areas of considerable vibrations are practical examples of components that might be subjected to several millions of cycles of stress in a relatively short period of time. For a vibration frequency of only 6 cycles per second, such a component will undergo over one million reversals of stress in a period of two days.

This investigation attempts to take a step in the direction of defining the fatigue properties of a glass-reinforced plastic by experimentally determining the fatigue characteristics of a particular laminate configuration which might be used in the construction of a ship hull. More specifically, the goals of this study are to;

      1. define the S-N curve for a hull construction type of composite,

      2. determine the fatigue crack propagation rate as a function of stress intensity factor for the same material,

3. determine the effect, if any, of a salt water environment on both the S-N curve and the fatigue crack propagation rate, and

4. develop a means of predicting the crack propagation rate from the data contained in the S-N curve.

A study of the fatigue properties of crossplied Scotchply (a high performance, high volume fraction, pre-preg, uni-directional ply, glass-reinforced epoxy) laminates by Mandell and Meier (4) showed that, for that material, crack growth rate varied approximately with the eleventh power of stress intensity factor. In Scotchply it was noted that a fatigue crack grows by propagating rapidly through a discrete "ligament" of the composite and then remaining at one position for many cycles before propagating through another ligament. (This is in contrast to the case for metals in which a fatigue crack grows a minute amount on every cycle.) A simple theoretical prediction of the crack growth rate from the fracture toughness, ultimate tensile strength and S-N curve for the unnotched material yielded an exponential relationship between crack growth rate and stress intensity factor which was in good agreement with the experimental data.

The composite chosen for the present study is considerably more complex than Scotchply in physical make-up. However, the same basic method is employed to analyze the experimental data and to display the results as was used

in the Mandell-Meier study. The purpose of this approach
is to attempt to determine if the proposed theory might be
more widely applicable than to Scotchply alone. An un-
notched, dogbone-shaped specimen is used to define the S-N
curves for both the air and salt water environments. A
specially-designed, "index card" specimen is used for the
determination of crack propagation rate in both the air and
salt water environments. The index card is also analyzed
for K-calibration and the dogbone specimen is used to deter-
mine Young's Modulus.

# II.  MATERIALS

In fabricating the specimens for this investigation,
an attempt was made to simulate an actual production method
that might be used in constructing a medium-sized boat of
the same material.  Details of the fabrication procedure
and particulars of the materials can be found in Appendix C.

The composite plates were prepared in 30" by 38"
sections using alternate layers of chopped fiber, random
mat glass and woven roving glass fabric in a matrix of
polyester resin.  Methyl ethyl ketone peroxide was used as
the curing catalyst.

In the early stages of the experimental portion of the
work, a laminate consisting of three layers of chopped mat
and two layers of woven roving was used.  The specimen
chosen for determining crack propagation rate was a 3" by
10" double edge-notched specimen.  This specimen type had
to be abandoned when it was found that the crack always
propagated too rapidly to permit measurement of the rate.
A 3" by 5", index card specimen was substituted but was
also found to be unsuitable because it buckled under load.
The configuration was then changed to one requiring five
layers of chopped mat and four layers of woven roving.
Both the notched and unnotched specimens of this construction
proved satisfactory.  A volume fraction of about 30% was
desired and was roughly controlled by controlling plate
thickness during fabrication.  Burn tests conducted on four

representative one-inch squares from the three plates re-
vealed an average actual volume fraction of 30.45%.

The plates were made using a standard, hand-lay-up
technique and were cured in air with no heat or pressure
applied. The plates were then cut into specimens and the
specimens were machined to final dimensions as described
in Appendix C. The geometry of both specimens is shown in
Figure 2.

The salt water used for both the presoak bath and the
testing environment was manufactured as needed using dis-
tilled water and 3% by weight of sodium chloride (C.P.
granular - Mallinckrodt Chemical Works). The solution was
usually made in batches consisting of 4000 ml of distilled
water and 124 grams of Na Cl.

## III.   EXPERIMENTAL PROCEDURE

A fatigue stress cycle is completely defined by speci-
fying any two of the four possible parameters of the cycle-
the maximum stress, the minimum stress, the mean stress and
the stress range.  The Instron Model 1211 Dynamic Cycler,
which was to be used for all fatigue testing, permits the
operator to pre-set the mean load and any one of the re-
maining three parameters in terms of loads - the resulting
stresses being determined simply by dividing the load by
the cross-sectional area of the specimen.  All specimens
were to be tested in tension-tension stress cycles.  If the
minimum load were allowed to go to zero, the grip assemblies
would slacken and motion of the specimen would result.
Therefore, it was decided that the minimum load in all
stress cycles would be standardized at 80 pounds for the
index card specimens and at 400 pounds for the dogbone
specimens; these specific loads were chosen because they
both represent 4% of the full range load scales used.  The
problem of specimen motion was thereby eliminated.  Tables
1a and 1b give the specifications for the ten loading condi-
tions used in the tests.  The machine was set up for 2000
pounds full scale load for the index card specimens and for
10,000 pounds full scale load for the dogbone specimens.
The two parameters used for controlling the tests were the
mean load and the load range (the fatigue cycle was load-
controlled).

In order to determine suitable load cycles for the fatigue tests, it was intended to find the ultimate load that could be sustained by each type of specimen and establish fatigue cycles in which the maximum loads were various fractions of the ultimate loads. The composite was known to be rate-sensitive and it was desired to test for ultimate load at approximately the same rate as would be achieved in the fatigue tests. Both the Instron Universal Testing Machine and the Instron Model 1211 Dynamic Cycler were used to obtain initial indications of ultimate loads. Neither of these machines, however, was capable of reaching the required rate. Therefore, actual values of ultimate loads were not determined until after fatigue tests were completed when an Instron Universal Static/Dynamic Testing Instrument Model 1250 was made available by Instron Corporation at their Canton, Massachusetts facility. Thus, the fatigue stress cycles used were based on the estimates of ultimate loads found from testing in air on the IUTM and the Model 1211. The estimated ultimate loads were 9200 pounds for the unnotched specimens and 1200 pounds for the notched specimens. The same loading conditions were applied to tests in both air and salt water.

Preliminary fatigue testing to determine practical limits on stress cycles indicated that for a stress cycle in which the maximum load was less than about 40% of the estimated ultimate load the time required to test to failure was excessive (on the order of $10^7$ cycles). This

resulted from the fact that all testing was to be done at
a frequency of 6 cycles per second. At higher frequencies,
the material heated up noticeably and at sufficiently high
frequencies the material would actually burn because of
internal friction. Similarly, for a stress cycle in which
the maximum load was greater than about 80% of the estimated
ultimate load the specimen failed so rapidly that an accur-
ate determination of the number of cycles to failure was
virtually impossible. Based upon these preliminary tests,
fatigue stress cycles were chosen in which the maximum loads
were 40%, 50%, 60%, 70% and 80% of the estimated ultimate
loads. The corresponding values of maximum load ranged
from 3680 to 7360 pounds for the unnotched specimens and
from 480 to 960 pounds for the notched specimens.

A description of all major apparatus used can be found
in Appendix D. The set-up procedure for all tests was
basically the same. In the case of the tests in salt water,
the salt water containment system was first installed on
the Dynamic Cycler. The salt water box was filled with
sodium chloride solution to a level sufficient to complete-
ly cover the specimen. In anticipation of the effect of
salt water on the metal parts required for gripping the
specimens, all parts that would come in contact with salt
water were either chrome-plated or made of brass or stain-
less steel. As a result of wearing and chipping of the
chrome plate, however, substantial corrosion of the base
metal (low-carbon steel) took place - particularly in the

later tests. This was manifested in the form of rather profuse amounts of a rust-colored precipitate. The amount of this precipitate was kept to a minimum by changing the water frequently. No attempt was made to analyze the precipitate nor to determine its effect, if any, on the tests.

In preparation for each test, the Dynamic Cycler was zeroed, balanced and calibrated in accordance with the technical manual. The stress cycle was set by adjusting the PRE-LOAD dial to the appropriate mean load and by placing the FUNCTION switch to the $\Delta$-LOAD position and adjusting the dial to the appropriate load range. The cycler was turned on and the frequency was checked to insure that the Hz meter always showed 7 Hz. (This reading on the Hz meter corresponded to an actual frequency of 5.93 Hz as determined from timing the frequency counter over about 500,000 cycles on several, separate occasions.) The ram position required to maintain the load cycle was controlled automatically by depressing the AUTO button in the STROKE CONTROL section of the panel.

Data-taking from the unnotched specimens consisted simply of noting the number of cycles to failure for each specimen. This information, together with the nominal maximum stress on the specimen, was sufficient to define the S-N curves for both the air and salt water environments. Three specimens were tested at each stress cycle for both the air and salt water environments.

The notched specimens were marked with lines perpendi-

cular to the notch at one-eighth inch intervals to facili-
tate determination of the location of the crack tip.  The
single biggest problem in the experimental work was the
accurate location of the crack tip.  The surface crack
was not considered to be a reliable indication because
significant debonding of individual fibers in the outside
layers of random mat confused the appearance of the crack
to such an extent that this method was discarded.  The
method eventually accepted resulted from a visual correla-
tion between the location of the crack tip as indicated
photo-elastically by cross-polarized light and the location
as determined by cutting several specimens progressively
closer to the surface crack tip until the specimens easily
parted into two pieces.  Comparison of the two locations of
the crack tip suggested that viewing the crack through
polarized light while the specimen was under load gave the
crack tip location as the beginning of the dark interference
band near the crack tip.  Though this method was recognized
as being imperfect it was employed to obtain all crack
growth rate data.  The accepted crack tip location is shown
schematically in Figure 8.

The data-taking from the notched specimens consisted of
determining the location of the crack tip as accurately as
possible (considered to be to the nearest half-interval,
i.e., 1/16") and recording both the crack tip location and
the total number of cycles elapsed up to the time of that
determination.  Growth rate could then be found by dividing

the distance the crack advanced by the number of cycles required for that advance distance. A replication factor of three was again used for both the air and salt water environments.

A time schedule was established for those specimens that were to be presoaked in salt water prior to testing. The ten-day presoak period was measured from the time a specimen was inserted into the bath until the time it was installed in the Dynamic Cycler to begin testing, exclusive of the time required to perform the test. Thickness measurements and weights were taken prior to placing the specimens in the bath in order to discern whether or not any significant water absorption took place.

To determine the appropriate rate at which to test specimens for actual ultimate tensile strength, a static test was performed on one of each of the two specimen types. A large retaining nut (used to secure the salt water containment system to the Dynamic Cycler) was threaded into place and a specimen was installed. The PRE-LOAD dial was set to 400 pounds for the dogbone specimen or 80 pounds for the index card specimen ($P_{min}$ in the respective 60% load cycles) and the pin of a dial indicator was rested on the retaining nut. The dial indicator position was adjusted so that a deflection of about 0.3 inch was indicated with the minimum load applied. The PRE-LOAD dial was then adjusted to 5520 pounds for the dogbone specimen or 720 pounds for the index card specimen ($P_{max}$ in the respective

60% load cycles) and the change in dial indicator deflection between the two loading conditions for the two specimens was noted. Knowing this deflection and the frequency at which the fatigue tests were conducted the strain rate was determined from;

$$(2c \frac{in}{cyc})(f \frac{cyc}{sec})(60 \frac{sec}{min}) = \text{strain rate } \frac{in}{min},$$

where c is the deflection change from the dial indicator.

The strain rates thus obtained were 60 in/min for the dogbone specimen and 30 in/min for the index card specimen. Using the 60% load cycles was considered to provide average strain rates for all fatigue loading conditions. Tables 2a and 2b give the data acquired from ultimate strength tests.

# IV.  ANALYTICAL METHOD

One of the purposes in conducting this study was to
develop a means of predicting crack growth rate from
information contained in the S-N curve for the material.
With this in mind, the analysis was formulated in such a
way that the observed variation of crack growth rate with
stress intensity factor could be compared with the rela-
tionship between crack growth rate and stress intensity
factor as predicted by the theory developed by Mandell and
Meier for Scotchply.

The basis of the theory lies in the hypothesis that
the material at the tip of a crack will fail in fatigue
in accordance with the S-N curve for unnotched specimens
of the same material, the fatigue life being determined by
the local stress level at the crack tip.  Since the material
local to the crack tip must reach its local ultimate
tensile strength at the same time as the stress intensity
factor reaches the value of the candidate critical stress
intensity factor, it can be stated that;

$$\sigma_1 = \sigma_f \frac{K_I}{K_Q} . \qquad (1)$$

The assumption of linearity between $\sigma_1$ and $\sigma_f$ implied by
this equation is questioned by Mandell and Meier because
of the growth of the splits at the crack tip during the
fatigue process.  The initiation and growth of such splits
have been shown to be the source of fracture toughness in

composites of this type (6). The validity of the linearity
assumption might also be questioned in this instance, al-
though the growth of vertical splits was not as evident for
the material and geometry used for this investigation.

If the S-N curve for the unnotched material can be
defined (or at least approximated) by a straight line, its
equation can be written as;

$$\log N = \frac{\sigma_f - \sigma}{s} .$$
(2)

If, then, $\sigma_1$ from equation (1) is inserted into equation (2)
for $\sigma$, the result is;

$$\log N = \frac{\sigma_f}{s} \left( 1 - \frac{K_I}{K_Q} \right) .$$
(3)

To facilitate the prediction of crack growth rate, the
assumption is made that the effect of the stress distribu-
tion beyond the crack tip is negligible. For all crack
lengths, the stress immediately at the crack tip is taken
as that given by equation (1) and zero stress prevails
elsewhere. This assumption has the effect of neglecting
any cumulative damage that may occur ahead of the crack tip.
Mandell and Meier showed that , for ligament widths greater
than o.oo1 inch for Scotchply, neglecting the cumulative
damage effect introduced insignificant error. Additionally,
only a minor difference was noted between their predicted
curve neglecting cumulative damage and their curve account-
ing for cumulative damage over the first five ligaments
ahead of the crack tip.

The final assumption is made, based on experimental observation, that the mechanism of material failure is one of ligament advance - that is, the fatigue crack advances a distance d during a very small number of cycles and then remains at the new position for many cycles before advancing by another ligament width.

With this basis for the analysis established, crack growth rate can be found by dividing the distance d by the number of cycles given by equation (3);

$$\frac{da}{dN} = \frac{d}{\exp\ 2.3\left[\frac{\sigma_f}{s}\left(1-\frac{K_I}{K_Q}\right)\right]}\ . \qquad (4)$$

The important dimension d could only be found by observing the growth of the crack in the notched specimens during the fatigue tests. This task was quite difficult in the cases of both the very low and very high load cycles because of the problem of timing the observation to the very short interval when the crack propagated. Based on observations made during the tests on specimens loaded to 600, 720 and 840 pounds ($P_{max}$), a value of 0.125 inch was assigned to d.

In order to reduce the data for purposes of comparison with the relationship given by equation (4), two methods were employed. The first was based on the Irwin-Kies K-calibration tests (7) described in Appendix E. The stress intensity factor and crack propagation rate were evaluated within each loading cycle at each observed value

of crack length.  An average of about six data points were
provided by each of the notched index card specimens tested.

Boundary collocation K-calibration also has been found
to be useful in applications such as this (8).  Gross and
Srawley developed a fitting equation to boundary colloca-
tion results (9) which gives stress intensity factor as a
function of crack length, load and specimen geometry.
The equation,

$$\frac{KBH^{\frac{1}{2}}}{P} = 3.46 \left(\frac{a}{H} + 0.7\right), \qquad (5)$$

is specifically for the index card type of specimen (assum-
ing infinite specimen length) used in this work to obtain
crack growth rate data and thus might be expected to give
good results.  In applying equation (5), B and H were fixed
by the specimen geometry.  The equation then reduces to;

$$K = P(8.72\ a + 9.13). \qquad (6)$$

Values of crack length, a, and the maximum load in the
cycle under which a particular specimen was fatigued, $P_{max}$,
were inserted into equation (6) to provide values for K.
The values of crack growth rate again were the rates ob-
served during the experiments.

The candidate critical stress intensity factor, $K_Q$,
was validated as a material property by running a K-cali-
bration test similar to that described by Bowie (10) for
symmetrically edge-cracked specimens.  Three index card
specimens were tested in tension at a constant strain rate
(0.02 in/min).  As the crack extended from the notch, the

load at every one-eighth inch interval of growth was noted.
The Irwin-Kies formula was used to reduce the data. Inspec-
tion of Figure 10 shows that $K_Q$ varies relatively little
around the average value of about 17.5 ksi-in$^{\frac{1}{2}}$. The data
used to plot Figure 10 are given in Table 5.

The experimental results and their comparison with
theoretical behavior are displayed in Figures 12 through 15
in Appendix A. The data that produced these results are
given in Tables 6 through 11 in Appendix B.

## S-N Curves

The fatigue data from the unnotched specimens produced
non-linear S-N curves in the cases of both air and salt
water environments. For purposes of attempting to verify
the Mandell-Meier theory, the linear approximations shown
in Figures 12 and 13 were used. For the air environment,
the approximation gave a value for $\sigma_f$ of 31.0 ksi and a
value for the slope, s, of 3.48 ksi per decade of cycles.
In the case of the salt water environment, the linear app-
roximation gave a value for $\sigma_f$ of 27.0 ksi and a value for
the slope of 3.14 ksi per decade of cycles. These values
were used to plot the theoretical curves of $\frac{da}{dN}$ vs K in
Figures 14 and 15.

Comparison of the S-N curves for the two different en-
vironments shows a general, but moderate, tendency toward
decreased fatigue life for the salt water environment.
Alternatively, for a given number of cycles, a lower stress
can be withstood in salt water than in air. This is pointed
out by the 10% lower value of $\sigma_f$ in salt water. The per-
centage variation in slope between the two curves is about

equal to the percentage variation in $\sigma_f$ .

## Crack Propagation Rates

In Figures 14 and 15, the data for $\frac{da}{dN}$ vs K are plotted to compare with the curve given by the Mandell-Meier theory for fatigue behavior. It can be seen that substantial agreement exists between the theory and the experimental results. Because the experimental data reduced by both the Irwin-Kies and the Gross-Srawley methods gave essentially identical results, only the Irwin-Kies data points are plotted. Both the theoretical and experimental results indicate that crack growth rate is proportional to about the twelfth power of stress intensity factor, regardless of the environment. Comparison of Figures 14 and 15 also shows that the salt water environment shifts the curve and the data to the left (or up) by a constant amount along the length of the curve on the log-log plot.

## General

For a given crack length within a given fatigue load cycle, reduction of the data by the Irwin-Kies formula gave precisely the same values as reduction by the Gross-Srawley formula except at very long crack lengths, where the assumption of infinite specimen length for the Gross-Srawley case was violated.

No significant increase in either thickness or weight of

the specimens presoaked in salt water was observed indicating
that, at least for a ten-day presoak period, water absorp-
tion by the material was negligible.

# VI.  DISCUSSION OF RESULTS

Although the data obtained from the unnotched specimens
did not produce linear S-N curves, very close-fitting
straight lines could be passed through all of the data
points except the points representing the actual ultimate
tensile strengths.  When these linear approximations were
made, the straight lines were extrapolated to one cycle to
provide values of $\sigma_f$ for use in equation (4).  These
approximations can only be considered valid in the regions
where the actual curves and the straight lines are very
close.  In this instance, those regions covered all of the
data points other than the ultimate tensile strengths.

The fact that the S-N curves were not linear correlates
with previous observations (11) in which a sharp drop-off
in the S-N curve was noted.  This phenomenon is especially
pronounced for composites containing a polyester resin
matrix.  The conclusion to be drawn from the sharp drop is
that the first several cycles at high loads greatly degrade
the material thereby producing shorter fatigue lives than
might be hoped for from simply knowing the ultimate tensile
strength and expecting a linear curve.

Another factor bearing on the non-linearity of the S-N
curves in this particular case is provided by closer scruti-
ny of the manner in which the strain rate to be used for
the UTS tests was determined.  The fact that a static test

was employed to determine a dynamic parameter leaves the
method open to criticism. If the static test result gave
a strain rate that was too high, the resulting value of
UTS would be too high and some non-linearity would thus
be introduced.

Unfortunately, the absence of data between the UTS
and the highest stress levels at which fatigue tests were
conducted precluded further definition of the true curve
in this area. This was a result not only of the fact that
the true UTS values were not known until after the fatigue
tests were run but also of the difficulty that would be
encountered in attempting to find the number of cycles
in the very short fatigue lives at stress levels in the
empty region. The magnitude of the void of data can be
best appreciated by comparing the nominal maximum stress
in the highest fatigue stress cycle (about 22,700 psi dry)
with the ultimate tensile strength (about 40,000 psi dry).

In this regard, a constraint is imposed by the limited
capability of the Model 1211 to achieve the preset stroke
in a reasonable number of cycles. The Model 1211 is not
at all suitable for measurement of fatigue life when that
fatigue life is below several hundred cycles. The Model
1250 is the preferred machine for the lower cycle fatigue
tests.

The wet strength retention of this material was found
to be about 90%. This fits very well with data obtained on

a very similar type of composite used in a submarine fair-
water (12), which also showed a wet strength retention of
about 90% after eleven years of marine service life.

Because of the close agreement between the Irwin-Kies
and the boundary collocation K-calibrations, the Irwin-Kies
method is seen to be a useful tool in experiments utilizing
an index card type of specimen.

In view of the close agreement between the experimental
data and the Mandell-Meier theory, it appears that the
theory is confirmed for this material.  Indeed, the tempta-
tion is great to say that the theory is widely applicable
to a broad range of composite constructions since Scotchply
and the material used in this study differ so greatly.  It
is important to note that confirmation of the theory also
serves to justify the assumptions made and to confirm the
mechanism as one of ligament advance.

# VII. CONCLUSIONS

1. The material tested produced non-linear S-N curves in both air and salt water environments. This should be expected because a polyester resin matrix was used. Because of the possibility of an erroneous method having been employed to determine ultimate tensile strength, the full reason for the non-linearity is left unexplained. It is possible that the S-N curves would, in fact, have been more nearly linear if a lower strain rate were used in the UTS tests.

2. Salt water decreases the fatigue life of the material by variable amounts depending on the stress cycle. The effect is minimized at low stress levels.

3. The Irwin-Kies K-calibration method is a simple but useful tool for use in studies involving fracture toughness and fatigue properties.

4. The Model 1211 Dynamic Cycler is not suitable for fatigue testing at stress levels close to the ultimate tensile strength of the material. The faster response of the Model 1250 Static/Dynamic Testing Instrument makes it the preferred testing machine for low cycle fatigue.

5. The Mandell-Meier theory of fatigue crack propagation is a viable theory for application to a wide range of composite materials. Crack growth by ligament advance appears to be a valid mechanism for the fatigue behavior.

# VIII. RECOMMENDATIONS

The work contained in this study was intended only as
a preliminary step in developing a viable theoretical
approach to the fatigue performance of glass-plastic compo-
sites. The fact that the experimental results of this study
seem to confirm the pioneering work of Mandell and Meier is
indeed encouraging. That very confirmation, however,
carries with it the need for more and expanded testing pro-
grams conceived with the idea of attacking the theory from
a critical viewpoint in order to either firmly refute it
or to further refine it until it becomes widely accepted
and used.

Future programs in fatigue testing of composites, parti-
cularly those of complex configurations, should provide
for testing at a sufficient number of stress levels to
specify the S-N curve without ambiguity. The Wohler dia-
gram is the starting point for all fatigue study and should
be undeniably well-defined. Where time permits, very low
stress cycles should be included to determine whether or
not the material exhibits an endurance limit.

Research is needed into methods that would be suit-
able for accurate determination of the crack tip location
in those materials where uncertainty may exist. Methods
that might be considered are visual (including refinement
of the photoelastic technique used in this work), acoustic,
strain gages, crack opening displacement and others.

Early standardization of specimen sizes and shapes for composite fatigue testing would be of value in insuring reproducibility of tests and thus of results. Such standardization, of course, can only come about after meaningful testing of different sizes and shapes has been conducted. The need for additional testing programs is thus re-emphasized. The absence of a standard specimen caused a relatively long delay in data-gathering for this work.

The effects of various parameters which were not investigated in this study provide fertile ground for follow-on work. Specifically, since most GRP materials are quite rate-sensitive, the effect of varying the testing frequency should be investigated within the limits where results are not influenced by specimen heat-up.

Because a significant effect on fatigue properties was noted after a salt water presoak period of only ten days (a negligible length of time in the life of a ship) the effect of longer presoak periods should be pursued in some detail. It is recommended that periods of 30 days and longer be used in future studies. In this regard, it is further recommended that a standard, synthetic sea water solution be used instead of the 3% sodium chloride solution to account for the possible effect of any trace elements. A standard mixture that would probably be acceptable is Synthetic Sea Salt available from Dayno Sales Company of Lynn, Massachusetts.

# REFERENCES

1. "The GRP Minehunter", NAVAL RECORD, Oct., 1972.

2. F.J. McGarry and J.F. Mandell, "Fracture Toughness
   Studies of Fiber Reinforced Plastic Laminates", MIT,
   Dept. of Civil Engineering Report R72-5 (1972).

3. K. Masubuchi, Materials for Ocean Engineering, MIT
   Press, (1970).

4. J.F. Mandell and U. Meier, "Fatigue Crack Propagation
   in $0^{\circ}/90^{\circ}$ E-Glass/Epoxy Composites", to be published
   (1973).

5. R. Kashihara, Personal Communication, MIT, Dept. of
   Civil Engineering, Jan. 15, 1973.

6. J.F. Mandell and F.J. McGarry, "The Origins of Fracture
   Toughness in Fiber Reinforced Plastics: Model and
   Crossplied Laminate Studies", MIT, Dept. of Civil
   Engineering Report R72-11 (1972).

7. G.R. Irwin and J.A. Kies, WELDING JOURNAL, 1952,
   vol. 31, 95s.

8. J.E. Srawley and B. Gross, "Stress Intensity Factors
   for Crackline-Loaded Edge-Crack Specimens", NASA
   Technical Note D-3820 (1967).

9. B. Gross and J.E. Srawley, "Stress Intensity Factors
   by Boundary Collocation for Single-Edge-Notch Specimens
   Subject to Splitting Forces", NASA Technical Note
   D-3295 (1966).

10. D.L. Bowie, "Rectangular Tensile Sheet with Symmetric
    Edge Cracks", Paper 64-APM-3, ASME, (1964).

11. L.J. Broutman and R.H. Krock, Modern Composite Materials,
    Addison-Wesley, Reading, Mass., (1967), p. 404.

12. N. Fried and W.R. Graner, "Durability of Reinforced
    Plastic Structural Materials in Marine Service",
    MARINE TECHNOLOGY, July, 1966.

# APPENDICES

# APPENDIX A.

## FIGURES

WASTE

| A-1-1 | A-1-2 | A-1-3 | A-1-4 | A-1-5 | A-1-6 | A-1-7 | A-1-8 | A-1-9 |
|-------|-------|-------|-------|-------|-------|-------|-------|-------|
| A-2-1 | A-2-2 | A-2-3 | A-2-4 | A-2-5 | A-2-6 | A-2-7 | A-2-8 | A-2-9 |
| A-3-1 | A-3-2 | A-3-3 | A-3-4 | A-3-5 | A-3-6 | A-3-7 | A-3-8 | A-3-9 |
| A-4-1 | A-4-2 | A-4-3 | A-4-4 | A-4-5 | A-4-6 | A-4-7 | A-4-8 | A-4-9 |

WASTE

FIGURE 1a.    SPECIMEN NUMBERING - Plate A
(36 index card specimens)

WASTE

| B-1-1  | B-1-2  | B-1-3  |
|--------|--------|--------|
| B-2-1  | B-2-2  | B-2-3  |
| B-3-1  | B-3-2  | B-3-3  |
| B-4-1  | B-4-2  | B-4-3  |
| B-5-1  | B-5-2  | B-5-3  |
| B-6-1  | B-6-2  | B-6-3  |
| B-7-1  | B-7-2  | B-7-3  |
| B-8-1  | B-8-2  | B-8-3  |
| B-9-1  | B-9-2  | B-9-3  |
| B-10-1 | B-10-2 | B-10-3 |
| B-11-1 | B-11-2 | B-11-3 |
| B-12-1 | B-12-2 | B-12-3 |

WASTE

FIGURE 1b.    SPECIMEN NUMBERING - Plate B
(36 dogbone specimens)

| C-1-1 | C-1-2 | C-1-3 | C-1-4 | C-1-5 | C-1-6 | C-1-7 | C-1-8 | C-1-9 | C-1-10 | C-1-11 |
| C-2-1 | C-2-2 | C-2-3 | C-2-4 | C-2-5 | C-2-6 | C-2-7 | C-2-8 | C-2-9 | C-2-10 | C-2-11 |
| C-3-1 | C-3-2 | C-3-3 | C-3-4 | C-3-5 | C-3-6 | C-3-7 | C-3-8 | C-3-9 | C-3-10 | C-3-11 |

WASTE

| D-1-1 | D-1-2 | D-1-3 |
| D-2-1 | D-2-2 | D-2-3 |
| D-3-1 | D-3-2 | D-3-3 |
| D-4-1 | D-4-2 | D-4-3 |
| D-5-1 | D-5-2 | D-5-3 |
| D-6-1 | D-6-2 | D-6-3 |

WASTE

FIGURE 1c.    SPECIMEN NUMBERING - Plate C/D
             (33 index card and 18 dogbone specimens)

2.5"

10.0"

1.75"

1.5" (STRAIGHT)

1.75"

2.5"

1.5"

2.0"

UNNOTCHED
(Dogbone)

0.5"

0.625"

1.5"

0.025"

0.5" DIA.

3.0"

5.0"
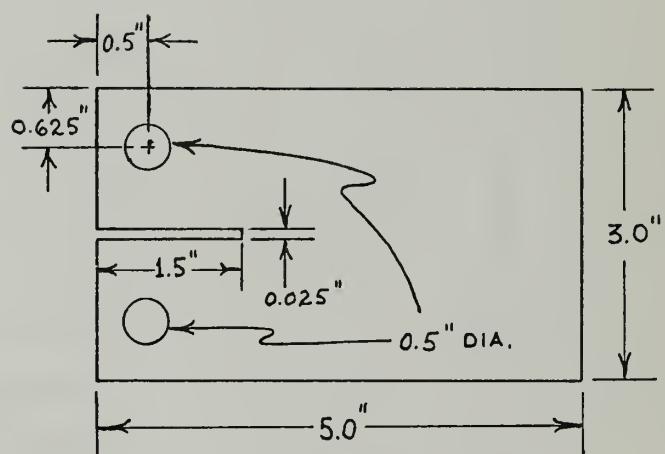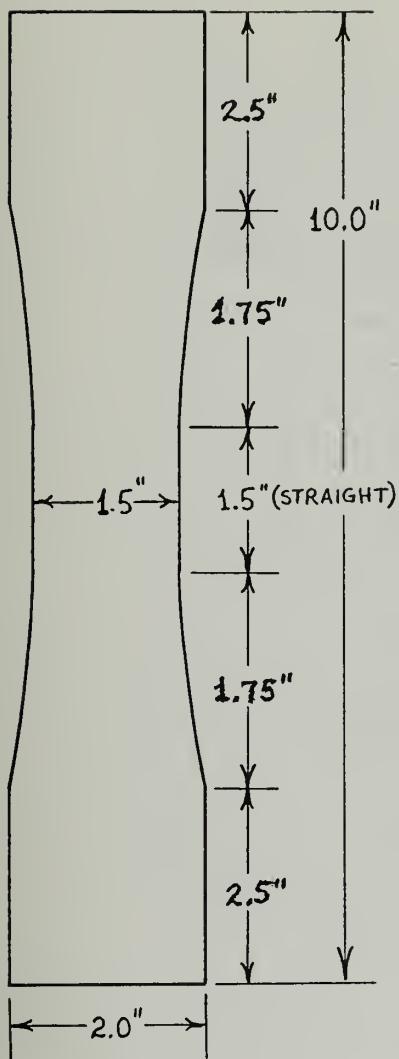
NOTCHED
(Index Card)

FIGURE 2.  FATIGUE SPECIMEN GEOMETRY
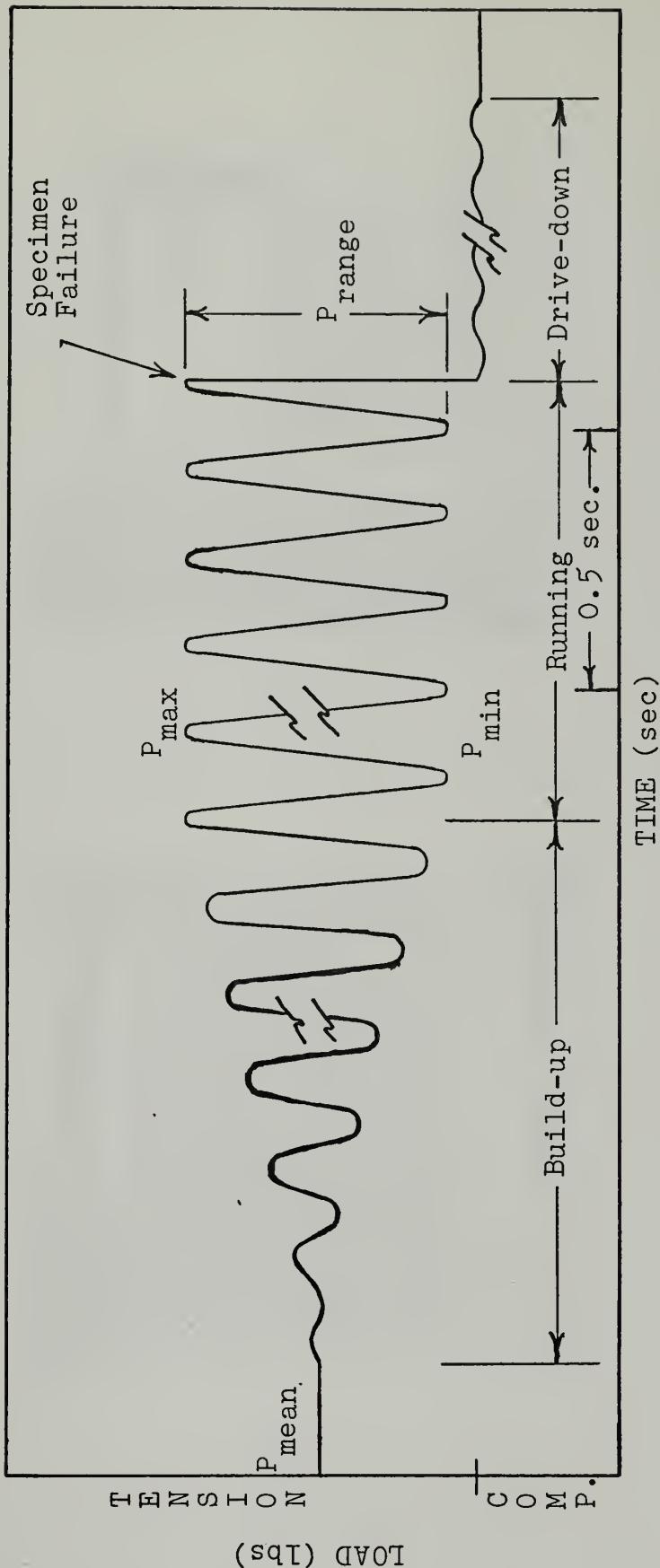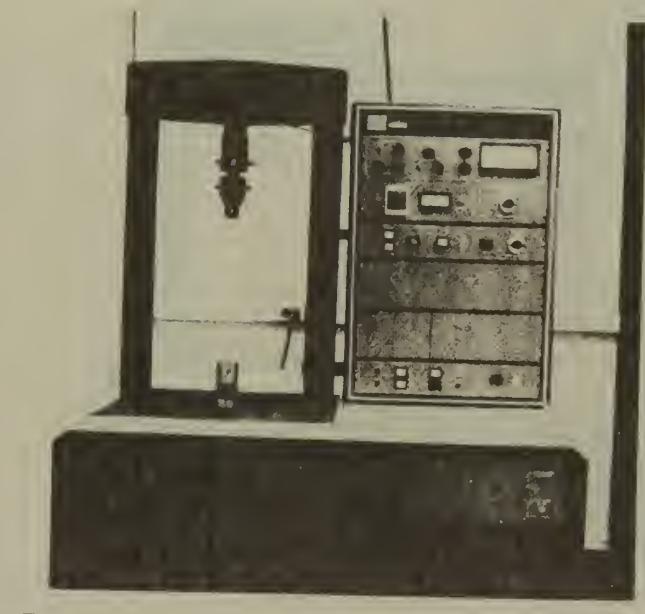
FIGURE 3. FATIGUE LOAD CYCLE CHARACTERISTICS
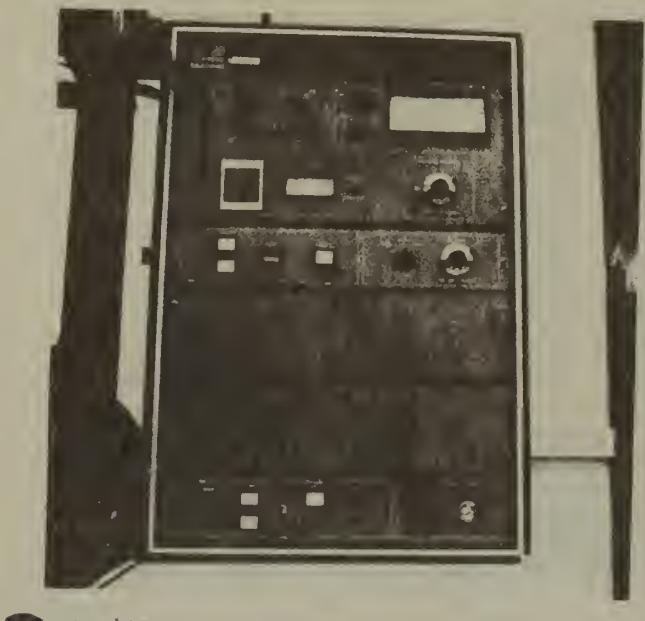
FIGURE 4a.

INSTRON MODEL 1211 DYNAMIC CYCLER



FIGURE 4b.

CONTROL PANEL OF MODEL 1211

FIG RE 4 .

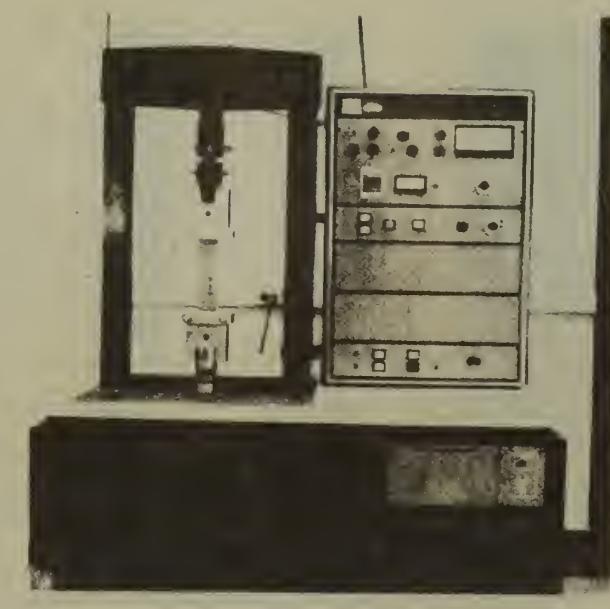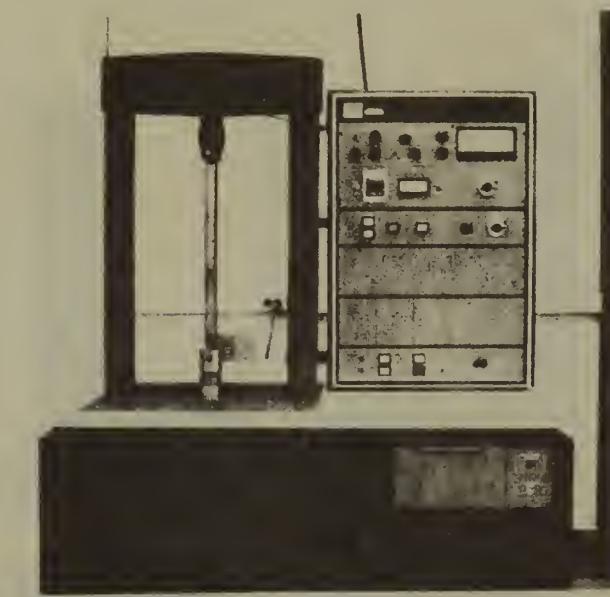MODEI 121 WITH UNNOTCHE DOG
SPECIMEN INSTAI ED



FI GURE 4d.
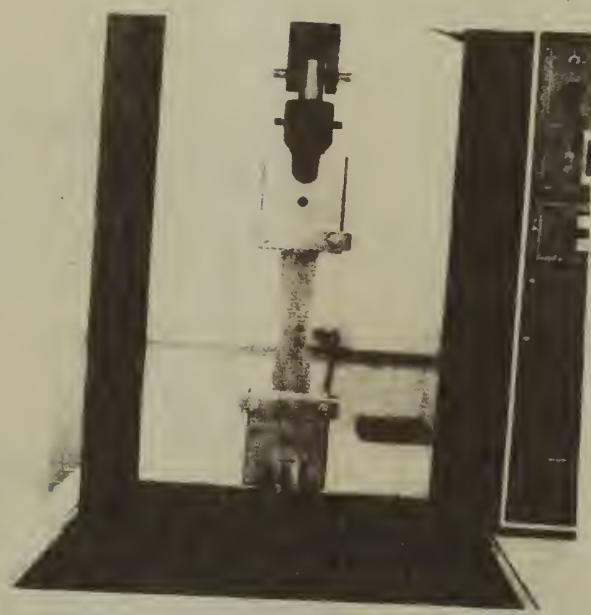
MODFL1211 WITH NOTCHED (INDEX CARD)
SPECIMEN INSTALLED
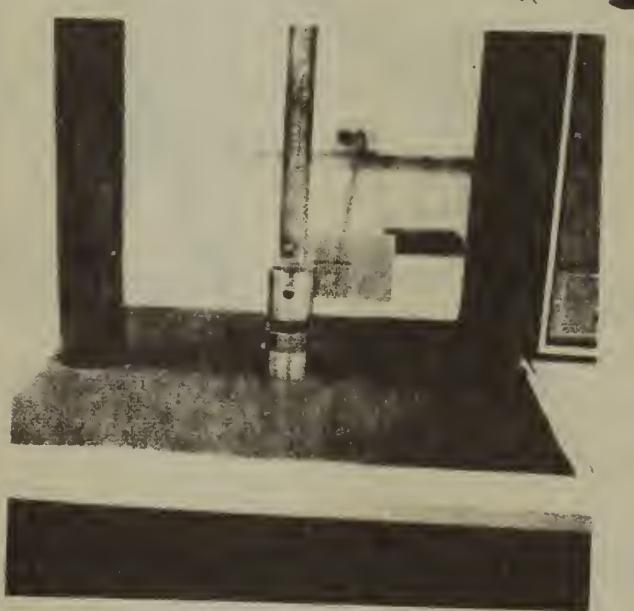
FIGURE 5a.

SPE IMEN GRIPPIN ASSE LY
( NNOTCHED SPECIMENS



F GUI 5..
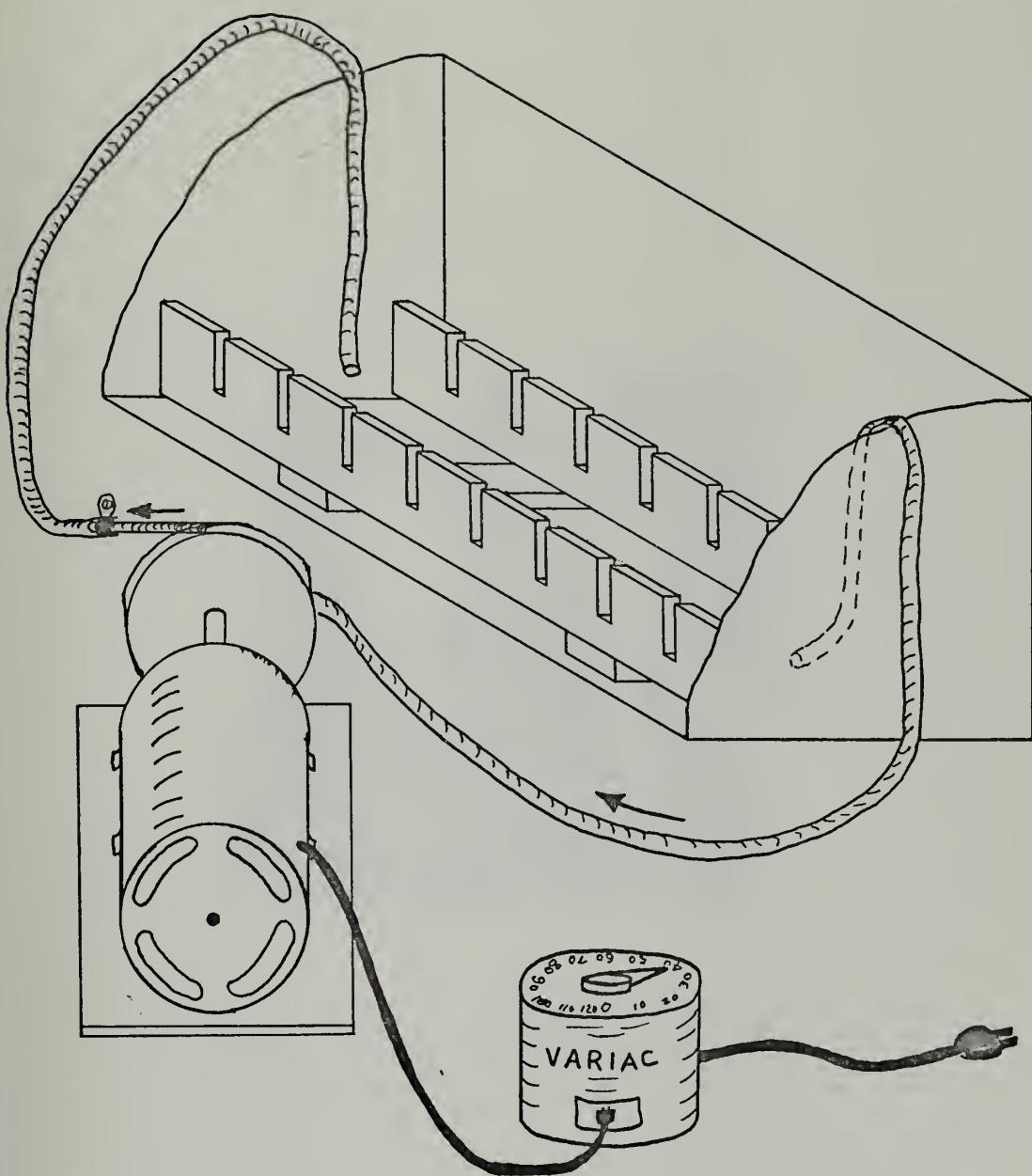
S ECIM N GRIP ING ASSEMBLY
(NO HE S ECIMENS)

FIGURE 6.   CIRCULATING SALT WATER PRESOAK BATH
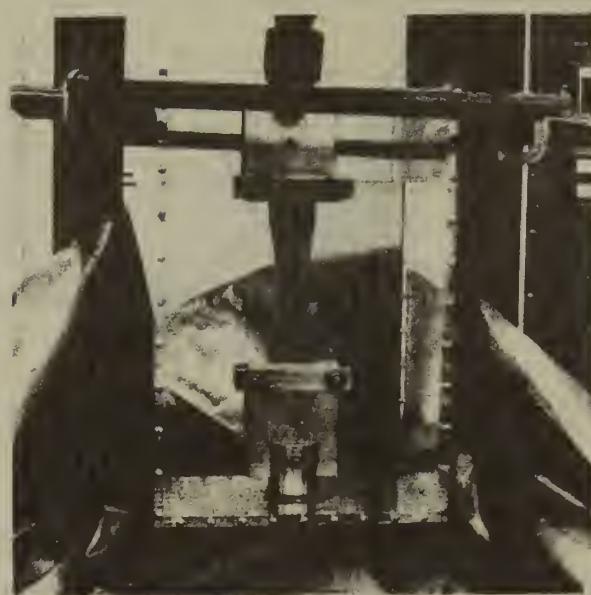
FIGURE 7.

SALT WATER CONTAINMENT SYSTEM
(SHOWN INSTALLED ON MODEL 1211)
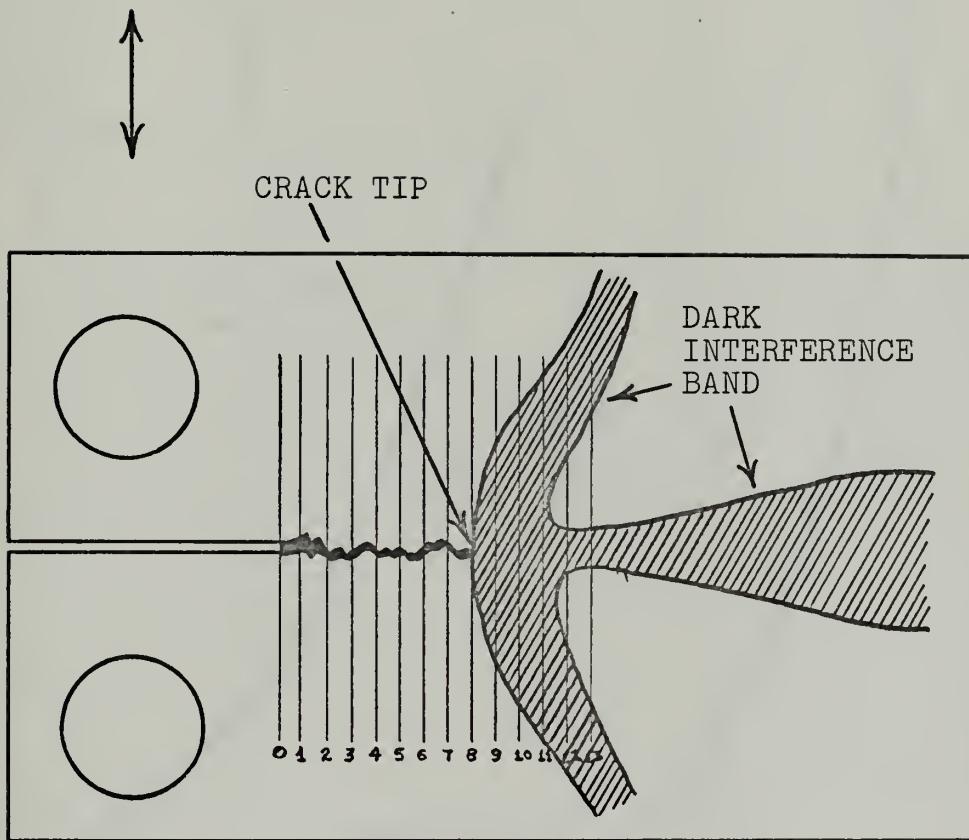
FIGURE 8.

LOCATION OF FATIGUE CRACK TIP
(SPECIMEN VIEWED THROUGH CROSS-POLARIZED LIGHT)
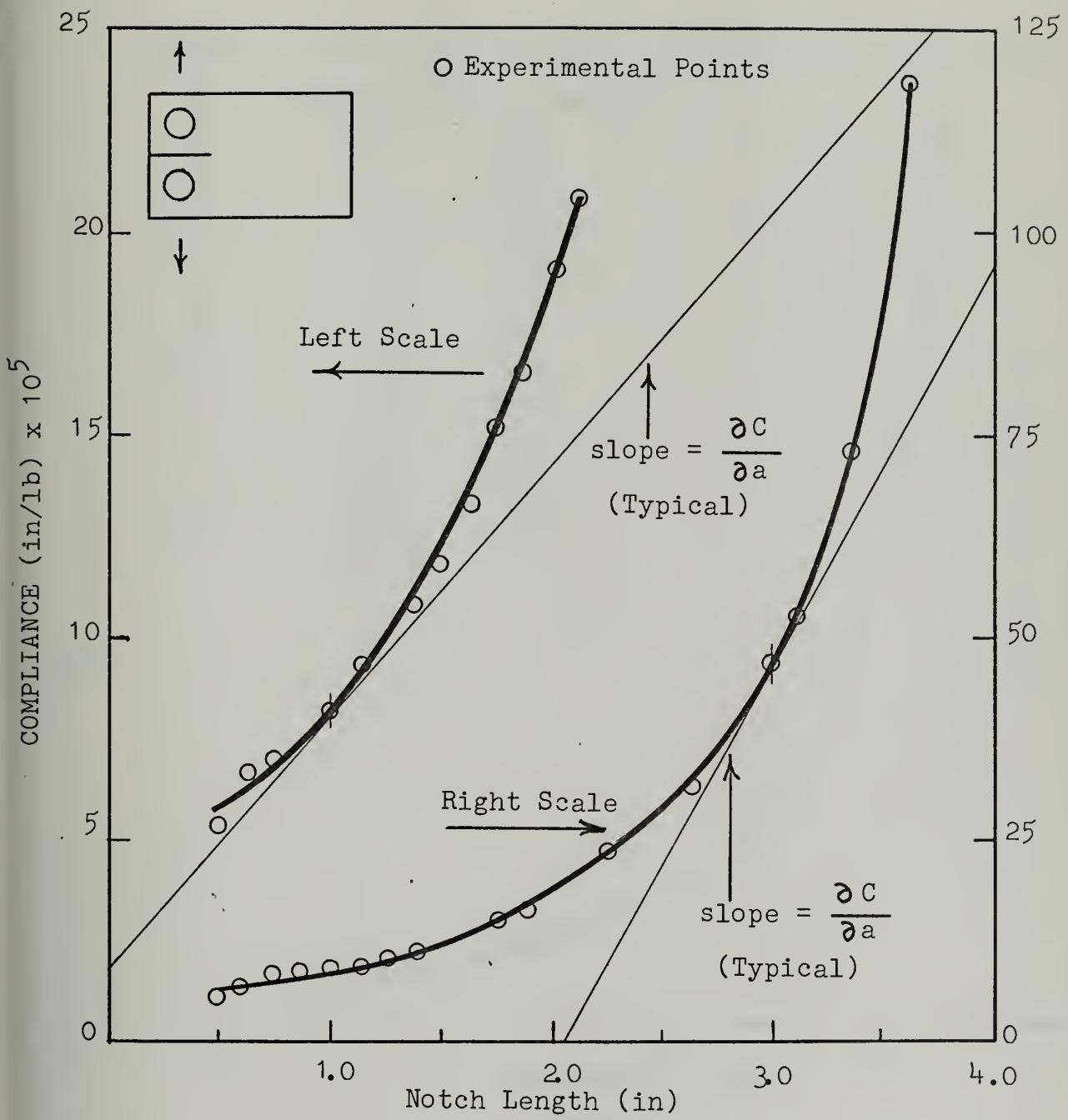
FIGURE 9.

COMPLIANCE VS NOTCH LENGTH FOR IRWIN-KIES K-CALIBRATION

-46-
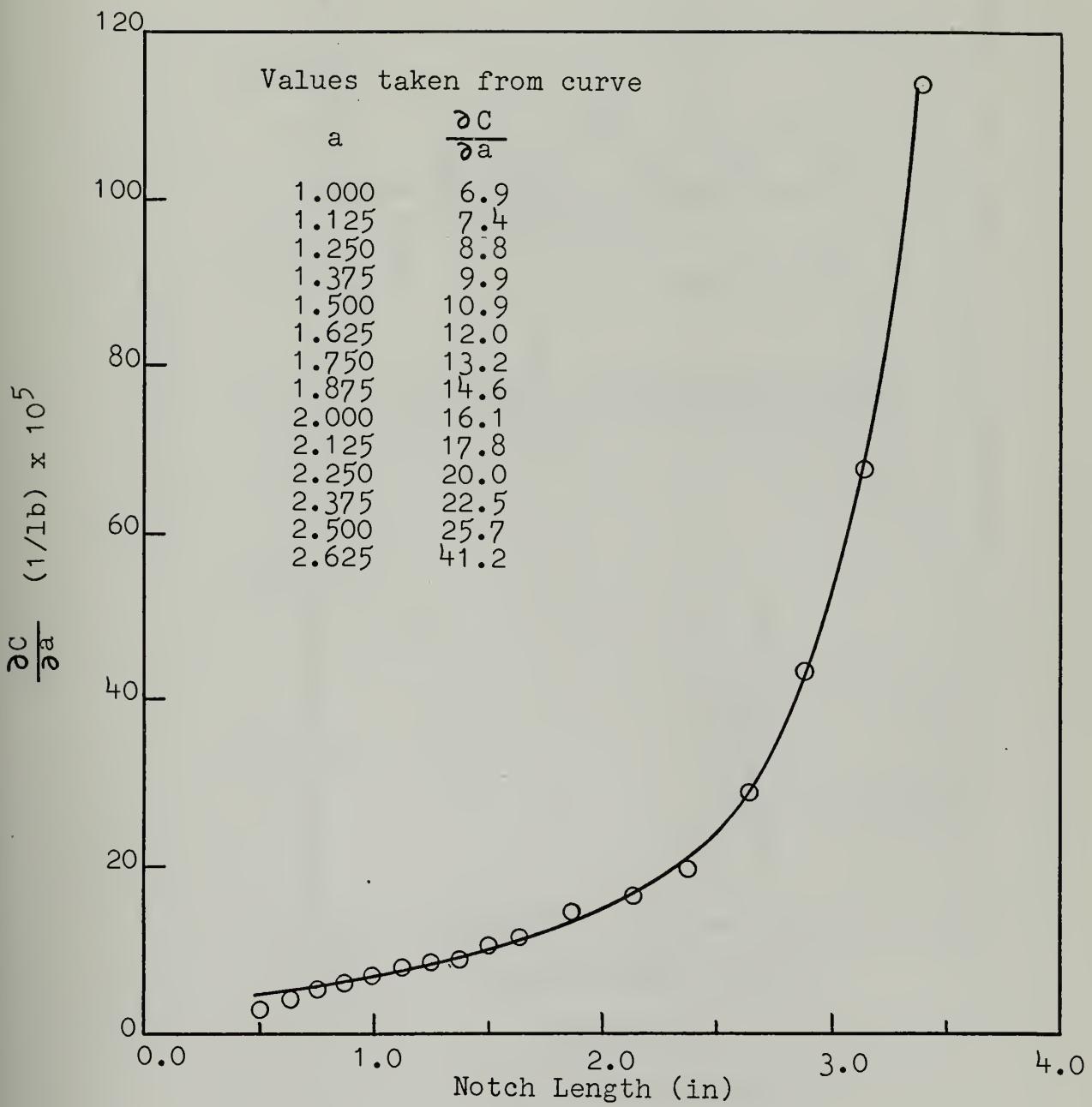
FIGURE 10.

$\dfrac{\partial C}{\partial a}$ VS NOTCH LENGTH FOR K-CALIBRATION
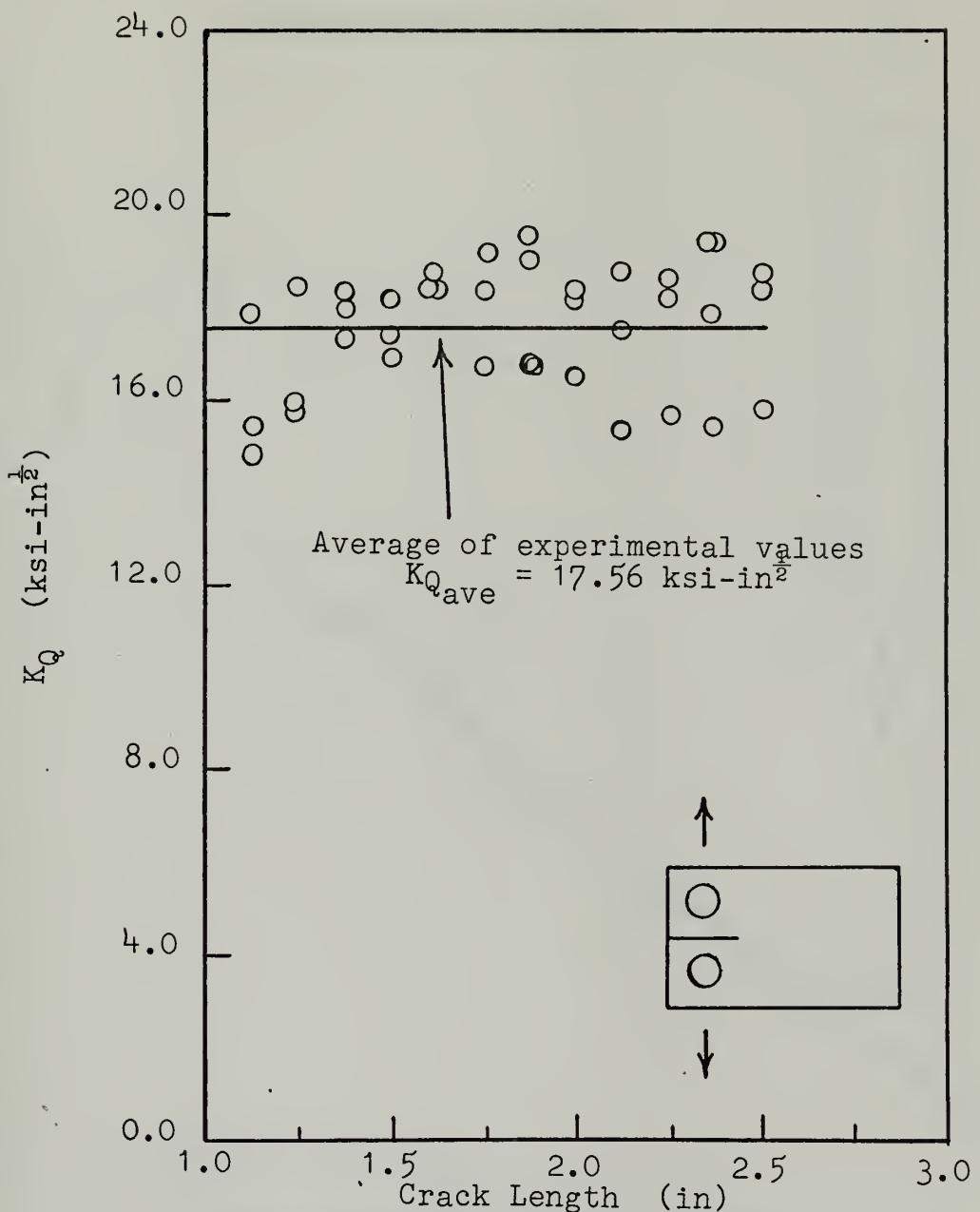
FIGURE 11.

$K_Q$ VS CRACK LENGTH

-48-
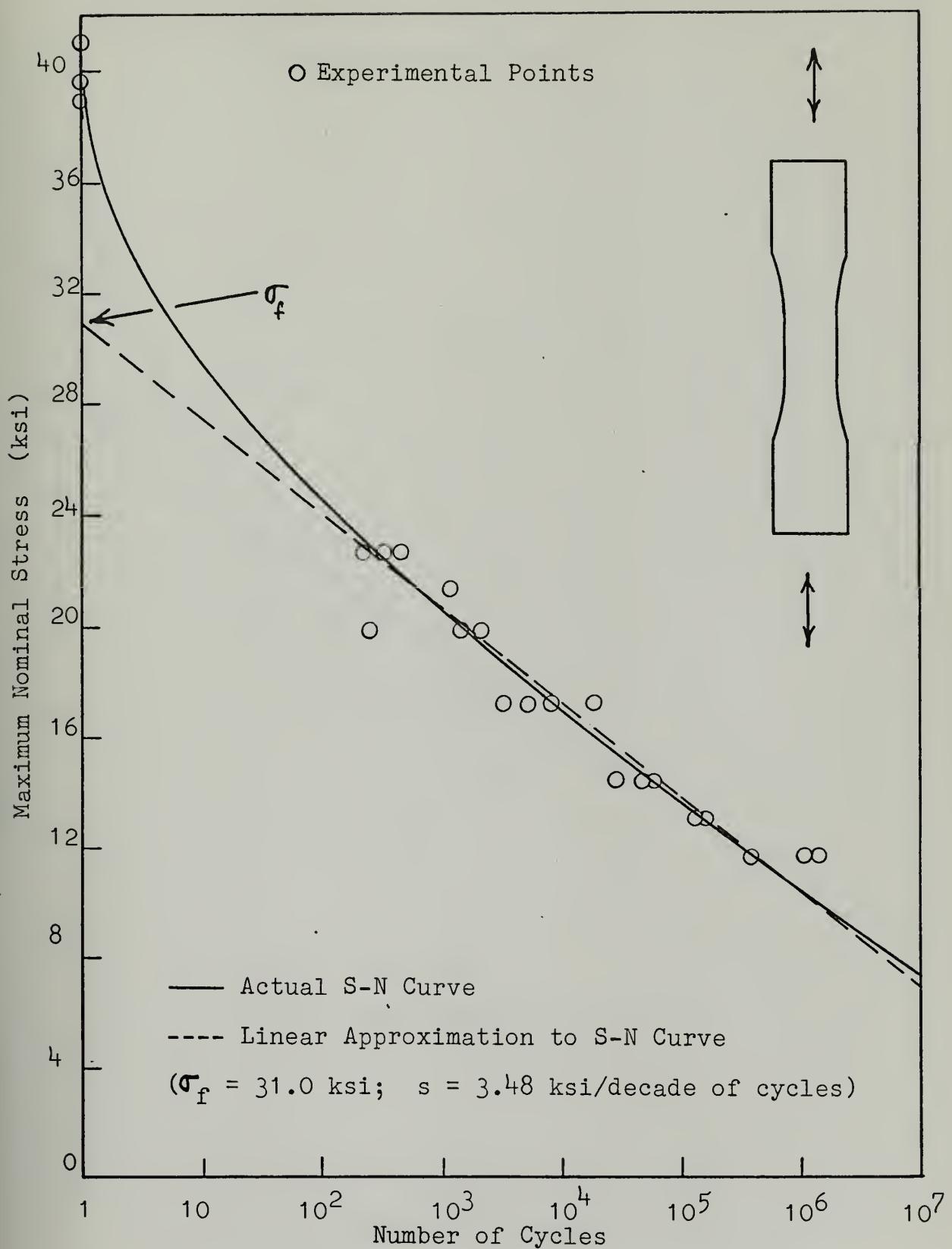
FIGURE 12. S-N CURVE (DRY ENVIRONMENT)
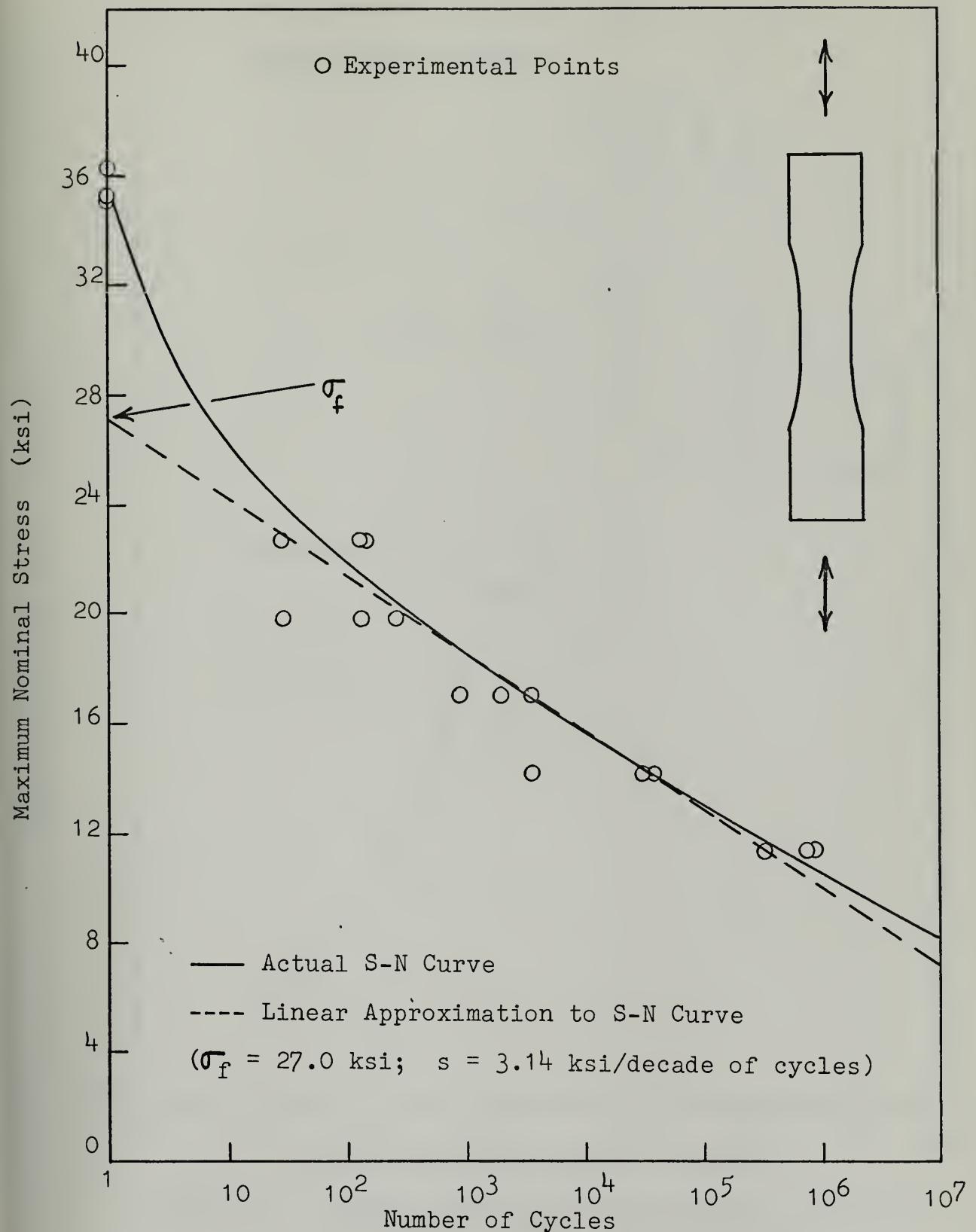
FIGURE 13. S-N CURVE (SALT WATER ENVIRONMENT)
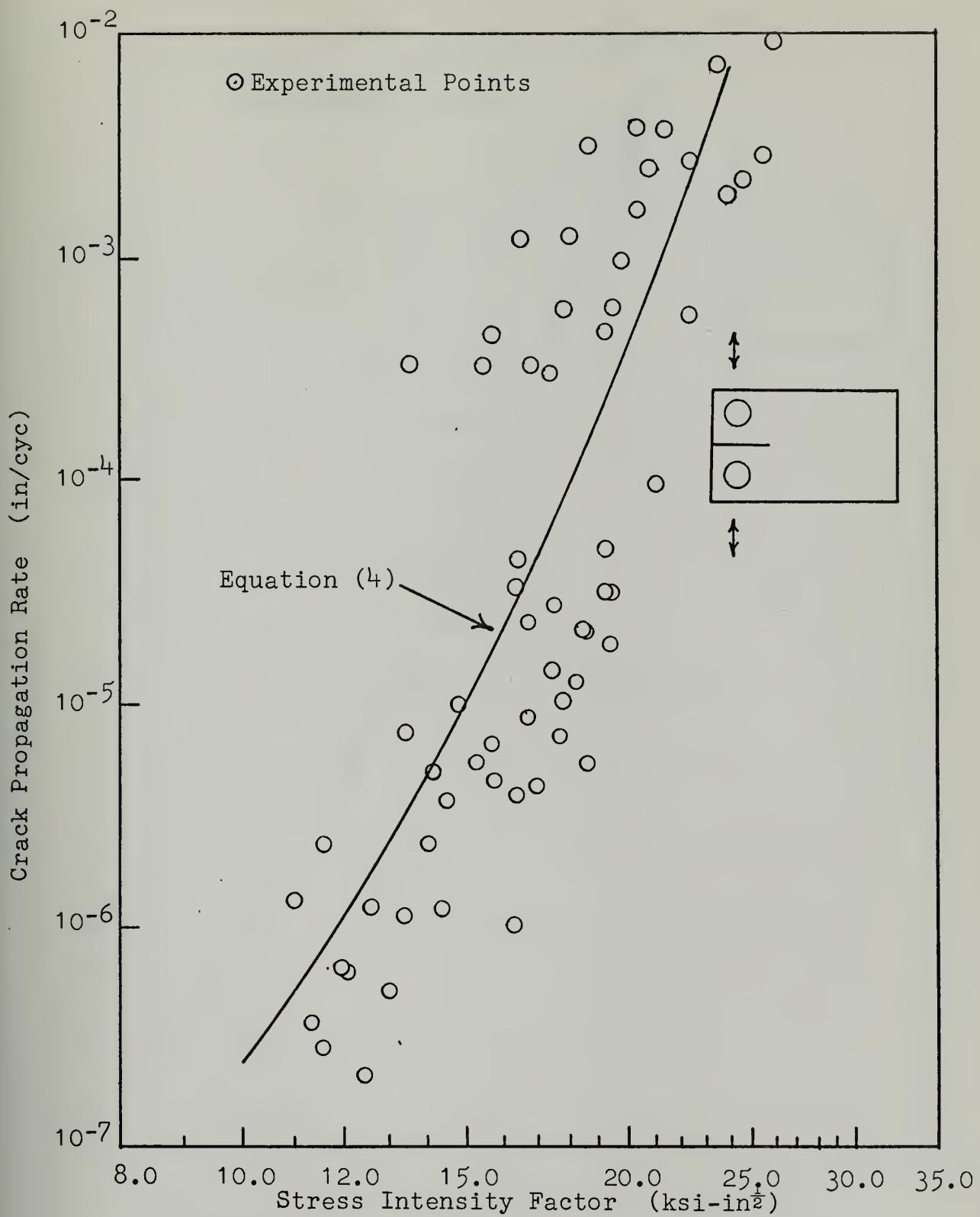
FIGURE 14. FATIGUE CRACK PROPAGATION RATE VS STRESS
INTENSITY FACTOR (DRY ENVIRONMENT)
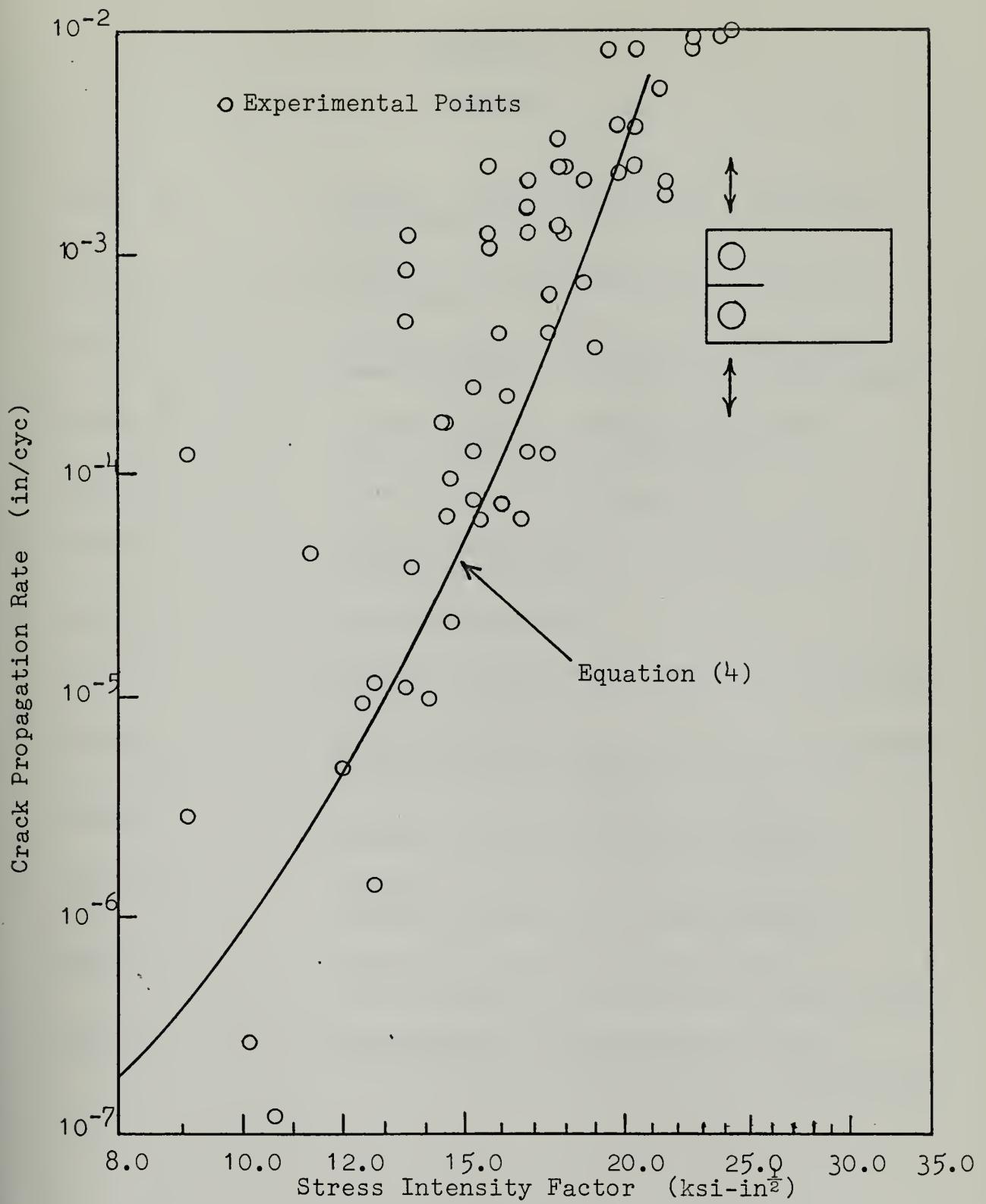
FIGURE 15. FATIGUE CRACK PROPAGATION RATE VS STRESS
INTENSITY FACTOR (SALT WATER ENVIRONMENT)

## APPENDIX B.

## TABLES

# TABLE 1a.

## FATIGUE LOADING CONDITIONS - UNNOTCHED SPECIMENS

(UTS$_{est}$ = 9200 lbs.  Load cycles are designated by;

$$\frac{P_{max}}{UTS_{est}} \times 100\%.)$$

| Load Cycle | 40% | 50% | 60% | 70% | 80% |
|---|---|---|---|---|---|
| $P_{max}$ | 3680 | 4600 | 5520 | 6440 | 7360 |
| $P_{min}$ | 400 | 400 | 400 | 400 | 400 |
| $P_{range}$ | 3280 | 4200 | 5120 | 6040 | 6960 |
| $P_{mean}$ | 2040 | 2500 | 2960 | 3420 | 3880 |

# TABLE 1b.

## FATIGUE LOADING CONDITIONS - NOTCHED SPECIMENS

(UTS$_{est}$ = 1200 lbs.  Load cycles are designated by;

$$\frac{P_{max}}{UTS_{est}} \times 100\%.)$$

| Load Cycle | 40% | 50% | 60% | 70% | 80% |
|---|---|---|---|---|---|
| $P_{max}$ | 480 | 600 | 720 | 840 | 960 |
| $P_{min}$ | 80 | 80 | 80 | 80 | 80 |
| $P_{range}$ | 400 | 520 | 640 | 760 | 880 |
| $P_{mean}$ | 280 | 340 | 400 | 460 | 520 |

TABLE 2a.

ULTIMATE TENSILE STRENGTH DATA - UNNOTCHED SPECIMENS

(Strain rate = 60 in/min)

| Specimen | Environment | Nominal Stress at Failure (psi) |
|----------|-------------|---------------------------------|
| B-2-2 | Dry | 41,148 |
| B-9-1 | Dry | 38,975 |
| B-3-2 | Dry | 39,654 |
| B-2-1 | Salt Water | 36,123 |
| B-7-1 | Salt Water | 35,105 |
| D-5-1 | Salt Water | 35,309 |

$$\frac{\text{Average S.W. UTS}}{\text{Average Dry UTS}} = 0.89$$

TABLE 2b.

ULTIMATE SUSTAINED LOAD - NOTCHED SPECIMENS

(Strain rate = 30 in/min.  Notch length - 1.0 inch from line of load application.)

| Specimen | Environment | Load at Failure (lbs) | $K_Q$ (ksi-in$^{\frac{1}{2}}$) from eq. (6) |
|----------|-------------|-----------------------|---------------------------------------------|
| C-1-8 | Dry | 1606 | 28.7 |
| C-2-2 | Dry | 1439 | 25.7 |
| C-2-5 | Dry | 1518 | 27.1 |
| C-3-5 | Dry | 1661 | 29.6 |
| C-1-5 | Salt Water | 1408 | 25.1 |
| C-2-6 | Salt Water | 1408 | 25.1 |
| C-2-11 | Salt Water | 1338 | 23.9 |

-55-

## TABLE 3.

### IRWIN-KIES K-CALIBRATION DATA

| Notch Length $a$ (in) | Average Compliance $C_{ave}$ (in/lb) $\times 10^5$ | $\frac{\partial C}{\partial a}$ (1/lb) $\times 10^5$ |
|---|---|---|
| 0.500 | 5.29 | 3.66 |
| 0.625 | 6.66 | 4.54 |
| 0.750 | 6.95 | 5.24 |
| 0.875 | 7.29 | 5.77 |
| 1.000 | 8.22 | 6.67 |
| 1.125 | 9.28 | 7.39 |
| 1.250 | 10.1 | 8.50 |
| 1.375 | 10.8 | 9.60 |
| 1.500 | 11.8 | 10.7 |
| 1.625 | 13.2 | 12.0 |
| 1.875 | 16.4 | 15.0 |
| 2.125 | 20.8 | 17.1 |
| 2.375 | 25.4 | 20.1 |
| 2.625 | 32.0 | 29.5 |
| 2.875 | 40.6 | 43.6 |
| 3.125 | 54.1 | 67.4 |
| 3.375 | 74.4 | 114 |

Specimens A-1-4, A-1-9 and A-3-9 were used
for this K-calibration.

# TABLE 4.

## BOUNDARY COLLOCATION K-CALIBRATION DATA

$$K = P(8.72a + 9.13)$$

| $P_{max}$ (lbs) (Load Cycle) | Crack Length (in) | $K$ (ksi-in$^{\frac{1}{2}}$) |
|---|---|---|
| 480 (40%) | 1.125 | 9.09 |
| | 1.250 | 9.62 |
| | 1.375 | 10.1 |
| | 1.500 | 10.7 |
| | 1.625 | 11.2 |
| | 1.750 | 11.7 |
| | 1.875 | 12.2 |
| | 2.000 | 12.8 |
| | 2.125 | 13.3 |
| | 2.250 | 13.8 |
| | 2.375 | 14.3 |
| | 2.500 | 14.9 |
| 600 (50%) | 1.125 | 11.4 |
| | 1.250 | 12.0 |
| | 1.375 | 12.7 |
| | 1.500 | 13.3 |
| | 1.625 | 14.0 |
| | 1.750 | 14.6 |
| | 1.875 | 15.3 |
| | 2.000 | 15.9 |
| | 2.125 | 16.6 |
| | 2.250 | 17.2 |
| | 2.375 | 17.9 |
| | 2.500 | 18.6 |
| 720 (60%) | 1.125 | 13.6 |
| | 1.250 | 14.4 |
| | 1.375 | 15.2 |
| | 1.500 | 16.0 |
| | 1.625 | 16.8 |
| | 1.750 | 17.6 |
| | 1.875 | 18.3 |
| | 2.000 | 19.1 |
| | 2.125 | 19.9 |
| | 2.250 | 20.7 |
| | 2.375 | 21.5 |
| | 2.500 | 22.3 |

TABLE 4.
(cont'd)

| $P_{max}$ (lbs) (Load Cycle) | Crack Length (in) | K (ksi-in$^{\frac{1}{2}}$) |
|---|---|---|
| 840 (70%) | 1.125 | 15.9 |
| | 1.250 | 16.8 |
| | 1.375 | 17.7 |
| | 1.500 | 18.6 |
| | 1.625 | 19.6 |
| | 1.750 | 20.5 |
| | 1.875 | 21.4 |
| | 2.000 | 22.3 |
| | 2.125 | 23.3 |
| | 2.250 | 24.1 |
| | 2.375 | 25.1 |
| | 2.500 | 26.0 |
| 960 (80%) | 1.125 | 18.2 |
| | 1.250 | 19.2 |
| | 1.375 | 20.3 |
| | 1.500 | 21.3 |
| | 1.625 | 22.4 |
| | 1.750 | 23.4 |
| | 1.875 | 24.5 |
| | 2.000 | 25.5 |
| | 2.125 | 26.5 |
| | 2.250 | 27.6 |
| | 2.375 | 28.6 |
| | 2.500 | 29.7 |

# TABLE 5

## $K_Q$-CALIBRATION DATA

| Specimen | Crack Length a (in) | Load P (lb) | $\frac{\partial C}{\partial a} \times 10^5$ (1/lb) | G (lb/in) | $K_Q$ (ksi-in$^{\frac{1}{2}}$) |
|---|---|---|---|---|---|
| C-1-6 | 1.125 | 950 | 7.8 | 163 | 17.8 |
| | 1.250 | 930 | 8.8 | 176 | 18.5 |
| | 1.375 | 850 | 9.9 | 166 | 18.0 |
| | 1.500 | 810 | 10.9 | 154 | 17.3 |
| | 1.625 | 790 | 12.0 | 173 | 18.4 |
| | 1.750 | 780 | 13.2 | 186 | 19.1 |
| | 1.875 | 740 | 14.6 | 185 | 19.0 |
| | 2.000 | 680 | 16.1 | 172 | 18.3 |
| | 2.125 | 620 | 17.8 | 158 | 17.5 |
| | 2.250 | 620 | 20.0 | 178 | 18.6 |
| | 2.375 | 610 | 22.5 | 194 | 19.4 |
| | 2.500 | 550 | 25.7 | 180 | 18.7 |
| C-2-1 | 1.125 | 790 | 7.8 | 113 | 14.8 |
| | 1.250 | 790 | 8.8 | 127 | 15.7 |
| | 1.375 | 820 | 9.9 | 154 | 17.3 |
| | 1.500 | 760 | 10.9 | 146 | 16.9 |
| | 1.625 | 790 | 12.0 | 173 | 18.4 |
| | 1.750 | 680 | 13.2 | 141 | 16.6 |
| | 1.875 | 650 | 14.6 | 143 | 16.7 |
| | 2.000 | 610 | 16.1 | 139 | 16.5 |
| | 2.125 | 540 | 17.8 | 120 | 15.3 |
| | 2.250 | 520 | 20.0 | 125 | 15.6 |
| | 2.375 | 480 | 22.5 | 120 | 15.3 |
| | 2.500 | 460 | 25.7 | 126 | 15.7 |
| C-2-8 | 1.125 | 820 | 7.8 | 121 | 15.4 |
| | 1.250 | 800 | 8.8 | 130 | 15.9 |
| | 1.375 | 870 | 9.9 | 173 | 18.4 |
| | 1.500 | 820 | 10.9 | 170 | 18.2 |
| | 1.625 | 800 | 12.0 | 178 | 18.6 |
| | 1.750 | 750 | 13.2 | 172 | 18.3 |
| | 1.875 | 760 | 14.6 | 195 | 19.5 |
| | 2.000 | 670 | 16.1 | 167 | 18.1 |
| | 2.125 | 660 | 17.8 | 179 | 18.7 |
| | 2.250 | 600 | 20.0 | 167 | 18.1 |
| | 2.375 | 600 | 22.5 | 188 | 19.3 |
| | 2.500 | 540 | 25.7 | 173 | 18.4 |

# TABLE 6

## FATIGUE FAILURE DATA - UNNOTCHED SPECIMENS

### (DRY ENVIRONMENT)

| Load Cycle | Maximum Nominal Stress (psi) | Specimen | Cycles to Failure |
|---|---|---|---|
| 40% | 11,358 | B-11-1 | 1,069,000 |
|  |  | B-12-2 | 1,606,000 |
|  |  | D-5-3 | 395,000 |
| 45% | 12,778 | B-3-3 | 128,000 |
|  |  | B-9-3 | 147,000 |
| 50% | 14,198 | B-9-2 | 72,900 |
|  |  | D-2-2 | 27,400 |
|  |  | D-2-3 | 38,600 |
| 60% | 17,037 | B-4-1 | 17,400 |
|  |  | B-5-1 | 8,750 |
|  |  | B-7-3 | 2,970 |
|  |  | B-1-2 | 5,450 |
| 70% | 19,877 | B-6-2 | 2,100 |
|  |  | D-3-3 | 1,490 |
|  |  | D-6-3 | 280 |
| 75% | 21,296 | B-4-3 | 1,300 |
| 80% | 22,716 | B-1-3 | 300 |
|  |  | D-1-1 | 240 |
|  |  | D-4-2 | 460 |

# TABLE 7

## FATIGUE FAILURE DATA - UNNOTCHED SPECIMENS

### (SALT WATER ENVIRONMENT AFTER 10-DAY SALT WATER PRESOAK)

| Load Cycle | Maximum Nominal Stress (psi) | Specimen | Cycles to Failure |
|---|---|---|---|
| 40% | 11,358 | B-1-1 | 576,000 |
|  |  | B-4-2 | 589,000 |
|  |  | B-7-2 | 320,000 |
| 50% | 14,198 | B-2-3 | 30,200 |
|  |  | B-5-2 | 38,700 |
|  |  | D-6-1 | 3,450 |
| 60% | 17,037 | B-12-1 | 910 |
|  |  | D-3-2 | 3,600 |
|  |  | D-4-1 | 2,070 |
| 70% | 19,877 | B-3-1 | 140 |
|  |  | D-1-3 | 270 |
|  |  | D-6-2 | 30 |
| 80% | 22,716 | B-8-2 | 140 |
|  |  | B-11-2 | 30 |
|  |  | B-12-3 | 140 |

# TABLE 8.

## THEORETICAL FATIGUE FAILURE DATA - NOTCHED SPECIMENS

### (DRY ENVIRONMENT)

$(\sigma_f = 31.0$ ksi; $s = 3.48$ ksi per decade of cycles;
$K_Q = 27.8$ ksi-in$^{\frac{1}{2}}$)

| $K$ (ksi-in$^{\frac{1}{2}}$) | $\exp\left[-2.3\dfrac{\sigma_f}{s}\left(1-\dfrac{K}{K_Q}\right)\right]$ (cycles) | $\dfrac{da}{dN}$ (in/cyc) |
|---|---|---|
| 10 | $2.0 \times 10^{-6}$ | $2.5 \times 10^{-7}$ |
| 11 | $4.4 \times 10^{-6}$ | $5.5 \times 10^{-7}$ |
| 12 | $8.3 \times 10^{-6}$ | $1.0 \times 10^{-6}$ |
| 13 | $1.8 \times 10^{-5}$ | $2.2 \times 10^{-6}$ |
| 14 | $3.6 \times 10^{-5}$ | $4.5 \times 10^{-6}$ |
| 15 | $8.0 \times 10^{-5}$ | $1.0 \times 10^{-5}$ |
| 16 | $1.8 \times 10^{-4}$ | $2.2 \times 10^{-5}$ |
| 17 | $3.4 \times 10^{-4}$ | $4.2 \times 10^{-5}$ |
| 18 | $7.7 \times 10^{-4}$ | $9.6 \times 10^{-5}$ |
| 19 | $1.4 \times 10^{-3}$ | $1.8 \times 10^{-4}$ |
| 20 | $3.2 \times 10^{-3}$ | $4.0 \times 10^{-4}$ |
| 21 | $7.2 \times 10^{-3}$ | $9.0 \times 10^{-4}$ |
| 22 | $1.4 \times 10^{-2}$ | $1.7 \times 10^{-3}$ |
| 23 | $3.1 \times 10^{-2}$ | $3.9 \times 10^{-3}$ |
| 24 | $5.6 \times 10^{-2}$ | $7.1 \times 10^{-3}$ |
| 25 | $1.3 \times 10^{-1}$ | $1.6 \times 10^{-2}$ |

## TABLE 9.

## EXPERIMENTAL FATIGUE FAILURE DATA - NOTCHED SPECIMENS

### (DRY ENVIRONMENT)

| Specimen (Load Cycle) | Crack Length (in) | Crack Growth Rate (in/cyc) | $K_1$ (ksi-in$^{\frac{1}{2}}$) |
|---|---|---|---|
| C-3-1 (50%) | 1.250 | $5.62 \times 10^{-7}$ | 12.0 |
| | 1.275 | $5.43 \times 10^{-7}$ | 12.1 |
| | 1.500 | $1.10 \times 10^{-6}$ | 13.3 |
| | 1.687 | $1.20 \times 10^{-6}$ | 14.3 |
| | 1.937 | $4.38 \times 10^{-6}$ | 15.8 |
| | 2.375 | $4.86 \times 10^{-5}$ | 19.1 |
| C-2-7 (50%) | 1.125 | $3.57 \times 10^{-7}$ | 11.3 |
| | 1.187 | $2.31 \times 10^{-6}$ | 11.6 |
| | 1.312 | $2.11 \times 10^{-7}$ | 12.4 |
| | 1.375 | $1.18 \times 10^{-6}$ | 12.7 |
| A-2-2 (50%) | 1.062 | $1.30 \times 10^{-6}$ | 11.0 |
| | 1.187 | $2.85 \times 10^{-7}$ | 11.6 |
| | 1.437 | $5.04 \times 10^{-7}$ | 13.0 |
| | 1.625 | $2.34 \times 10^{-6}$ | 14.0 |
| | 2.000 | $1.01 \times 10^{-6}$ | 16.2 |
| | 2.312 | $5.21 \times 10^{-6}$ | 18.6 |
| A-1-7 (60%) | 1.094 | $7.44 \times 10^{-6}$ | 13.3 |
| | 1.219 | $4.88 \times 10^{-6}$ | 14.1 |
| | 1.312 | $9.97 \times 10^{-6}$ | 14.8 |
| | 1.469 | $6.68 \times 10^{-6}$ | 15.7 |
| | 1.656 | $4.08 \times 10^{-6}$ | 17.0 |
| | 1.750 | $2.75 \times 10^{-5}$ | 17.5 |
| C-1-2 (60%) | 1.125 | $3.21 \times 10^{-5}$ | 13.5 |
| | 1.250 | $3.61 \times 10^{-6}$ | 14.4 |
| | 1.375 | $5.21 \times 10^{-6}$ | 15.2 |
| | 1.562 | $3.83 \times 10^{-6}$ | 16.3 |
| | 1.750 | $1.44 \times 10^{-5}$ | 17.5 |
| | 1.875 | $2.08 \times 10^{-5}$ | 18.5 |
| A-2-3 (70%) | 1.187 | $1.17 \times 10^{-3}$ | 16.3 |
| | 1.250 | $3.12 \times 10^{-4}$ | 16.8 |
| | 1.312 | $2.98 \times 10^{-4}$ | 17.3 |
| | 1.375 | $5.68 \times 10^{-4}$ | 17.8 |
| | 1.562 | $4.46 \times 10^{-4}$ | 19.1 |
| | 1.625 | $5.68 \times 10^{-4}$ | 19.5 |
| | 1.750 | $1.56 \times 10^{-3}$ | 20.5 |
| | 1.937 | $2.68 \times 10^{-3}$ | 22.2 |
| | 2.500 | $1.88 \times 10^{-2}$ | 28.6 |

TABLE 9.
(cont'd)

| Specimen (Load Cycle) | Crack Length (in) | Crack Growth Rate (in/cyc) | K ($ksi-in^{\frac{1}{2}}$) |
|---|---|---|---|
| C-1-9 (70%) | 1.125 | $4.17 \times 10^{-4}$ | 15.7 |
|  | 1.187 | $4.16 \times 10^{-5}$ | 16.3 |
|  | 1.250 | $2.31 \times 10^{-5}$ | 16.8 |
|  | 1.375 | $7.14 \times 10^{-6}$ | 17.8 |
|  | 1.437 | $1.25 \times 10^{-5}$ | 18.2 |
|  | 1.500 | $2.08 \times 10^{-5}$ | 18.6 |
|  | 1.625 | $1.78 \times 10^{-5}$ | 19.5 |
|  | 1.812 | $9.37 \times 10^{-5}$ | 21.0 |
|  | 2.250 | $2.92 \times 10^{-3}$ | 25.3 |
| C-2-3 (70%) | 1.062 | $3.12 \times 10^{-4}$ | 15.4 |
|  | 1.187 | $3.28 \times 10^{-5}$ | 16.3 |
|  | 1.250 | $7.81 \times 10^{-6}$ | 16.8 |
|  | 1.375 | $1.04 \times 10^{-5}$ | 17.8 |
|  | 1.562 | $3.12 \times 10^{-5}$ | 19.1 |
|  | 1.625 | $3.12 \times 10^{-5}$ | 19.5 |
|  | 1.937 | $5.21 \times 10^{-4}$ | 22.2 |
|  | 2.125 | $1.88 \times 10^{-3}$ | 23.8 |
| A-2-6 (80%) | 1.875 | $2.19 \times 10^{-3}$ | 24.6 |
| A-4-4 (80%) | 1.250 | $4.17 \times 10^{-3}$ | 19.2 |
|  | 1.500 | $1.25 \times 10^{-2}$ | 21.3 |
|  | 1.875 | $1.25 \times 10^{-2}$ | 24.6 |
|  | 2.625 | $1.88 \times 10^{-2}$ | 41.4 |
| C-2-9 (80%) | 1.125 | $1.25 \times 10^{-3}$ | 18.0 |
|  | 1.312 | $9.38 \times 10^{-4}$ | 19.8 |
|  | 1.437 | $2.50 \times 10^{-3}$ | 20.8 |
|  | 1.500 | $3.75 \times 10^{-3}$ | 21.3 |
|  | 2.000 | $9.38 \times 10^{-3}$ | 25.9 |
| C-3-2 (80%) | 1.187 | $3.12 \times 10^{-3}$ | 18.6 |
|  | 1.375 | $3.75 \times 10^{-3}$ | 20.3 |
|  | 1.750 | $7.50 \times 10^{-3}$ | 23.5 |
|  | 2.375 | $1.04 \times 10^{-2}$ | 30.6 |

# TABLE 10.

## THEORETICAL FATIGUE FAILURE DATA - NOTCHED SPECIMENS

### (SALT WATER ENVIRONMENT)

$(\sigma_f = 27.0$ ksi; $s = 3.14$ ksi pre decade of cycles;
$K_Q = 24.8$ ksi-in$^{\frac{1}{2}}$)

| $K$ (ksi-in$^{\frac{1}{2}}$) | $\exp\left[-2.3\dfrac{\sigma_f}{s}(1-\dfrac{K}{K_Q})\right]$ (cycles) | $\dfrac{da}{dN}$ (in/cyc) |
|---|---|---|
| 8 | $1.5 \times 10^{-6}$ | $1.9 \times 10^{-7}$ |
| 9 | $3.1 \times 10^{-6}$ | $3.8 \times 10^{-7}$ |
| 10 | $6.8 \times 10^{-6}$ | $8.4 \times 10^{-7}$ |
| 11 | $1.5 \times 10^{-5}$ | $1.8 \times 10^{-6}$ |
| 12 | $3.4 \times 10^{-5}$ | $4.2 \times 10^{-6}$ |
| 13 | $1.1 \times 10^{-4}$ | $1.4 \times 10^{-5}$ |
| 14 | $1.7 \times 10^{-4}$ | $2.1 \times 10^{-5}$ |
| 15 | $3.7 \times 10^{-4}$ | $4.6 \times 10^{-5}$ |
| 16 | $9.9 \times 10^{-4}$ | $1.2 \times 10^{-4}$ |
| 17 | $2.2 \times 10^{-3}$ | $2.7 \times 10^{-4}$ |
| 18 | $4.8 \times 10^{-3}$ | $6.0 \times 10^{-4}$ |
| 19 | $1.0 \times 10^{-2}$ | $1.3 \times 10^{-3}$ |
| 20 | $2.3 \times 10^{-2}$ | $2.9 \times 10^{-3}$ |
| 21 | $5.1 \times 10^{-2}$ | $6.4 \times 10^{-3}$ |
| 22 | $1.1 \times 10^{-1}$ | $1.4 \times 10^{-2}$ |

# TABLE 11.

## EXPERIMENTAL FATIGUE FAILURE DATA - NOTCHED SPECIMENS

### (SALT WATER ENVIRONMENT)

| Specimen (Load Cycle) | Crack Length (in) | Crack Growth Rate (in/cyc) | K (ksi-in$^{\frac{1}{2}}$) |
|---|---|---|---|
| C-3-6 (40%) | 1.125 | $2.78 \times 10^{-6}$ | 9.01 |
| | 1.375 | $2.60 \times 10^{-7}$ | 10.1 |
| | 1.500 | $1.21 \times 10^{-7}$ | 10.6 |
| C-1-1 (50%) | 1.125 | $1.25 \times 10^{-4}$ | 9.01 |
| | 1.312 | $9.10 \times 10^{-6}$ | 12.4 |
| | 1.375 | $1.13 \times 10^{-5}$ | 12.7 |
| | 1.562 | $3.75 \times 10^{-5}$ | 13.6 |
| | 1.750 | $9.37 \times 10^{-5}$ | 14.6 |
| | 2.000 | $2.27 \times 10^{-4}$ | 16.2 |
| C-3-7 (50%) | 1.125 | $4.16 \times 10^{-5}$ | 11.3 |
| | 1.250 | $4.60 \times 10^{-6}$ | 12.0 |
| | 1.375 | $1.40 \times 10^{-6}$ | 12.7 |
| | 1.500 | $1.04 \times 10^{-5}$ | 13.3 |
| | 1.625 | $9.60 \times 10^{-6}$ | 14.0 |
| | 1.750 | $2.08 \times 10^{-5}$ | 14.6 |
| | 1.875 | $6.25 \times 10^{-5}$ | 15.4 |
| | 2.062 | $6.25 \times 10^{-5}$ | 16.6 |
| | 2.187 | $1.25 \times 10^{-4}$ | 17.5 |
| C-1-4 (60%) | 1.125 | $1.25 \times 10^{-3}$ | 13.5 |
| | 1.250 | $6.57 \times 10^{-5}$ | 14.4 |
| | 1.375 | $2.50 \times 10^{-4}$ | 15.2 |
| | 1.750 | $6.58 \times 10^{-4}$ | 17.5 |
| | 2.250 | $1.79 \times 10^{-3}$ | 21.6 |
| C-3-3 (60%) | 1.125 | $8.33 \times 10^{-4}$ | 13.5 |
| | 1.250 | $1.67 \times 10^{-4}$ | 14.4 |
| | 1.375 | $7.81 \times 10^{-5}$ | 15.2 |
| | 1.500 | $7.35 \times 10^{-5}$ | 16.0 |
| | 1.625 | $1.25 \times 10^{-4}$ | 16.8 |
| | 1.750 | $4.17 \times 10^{-4}$ | 17.5 |
| | 1.937 | $3.75 \times 10^{-4}$ | 19.0 |
| | 2.250 | $2.08 \times 10^{-3}$ | 21.6 |
| C-3-10 (60%) | 1.125 | $5.00 \times 10^{-4}$ | 13.5 |
| | 1.250 | $1.67 \times 10^{-4}$ | 14.4 |
| | 1.375 | $1.25 \times 10^{-4}$ | 15.2 |
| | 1.500 | $4.17 \times 10^{-4}$ | 16.0 |
| | 1.625 | $1.25 \times 10^{-3}$ | 16.8 |
| | 2.125 | $2.50 \times 10^{-3}$ | 20.4 |

TABLE 11.
(cont'd)

| Specimen (Load Cycle) | Crack Length (in) | Crack Growth Rate (in/cyc) | $K$ $(ksi-in^{\frac{1}{2}})$ |
|---|---|---|---|
| A-1-5 | 1.125 | $1.25 \times 10^{-3}$ | 15.7 |
| (70%) | 1.250 | $2.08 \times 10^{-3}$ | 16.8 |
| | 1.375 | $2.50 \times 10^{-3}$ | 17.8 |
| | 1.625 | $8.33 \times 10^{-3}$ | 19.5 |
| | 2.000 | $9.38 \times 10^{-3}$ | 22.6 |
| A-3-5 | 1.125 | $2.50 \times 10^{-3}$ | 15.7 |
| (70%) | 1.375 | $1.39 \times 10^{-3}$ | 17.8 |
| | 1.500 | $7.35 \times 10^{-4}$ | 18.6 |
| | 1.750 | $3.57 \times 10^{-3}$ | 20.5 |
| | 2.125 | $9.38 \times 10^{-3}$ | 23.8 |
| A-4-8 | 1.125 | $1.04 \times 10^{-3}$ | 15.7 |
| (70%) | 1.250 | $1.56 \times 10^{-3}$ | 16.8 |
| | 1.375 | $3.12 \times 10^{-3}$ | 17.8 |
| | 1.500 | $2.08 \times 10^{-3}$ | 18.6 |
| | 1.750 | $8.33 \times 10^{-3}$ | 20.5 |
| | 2.000 | $8.33 \times 10^{-3}$ | 22.6 |
| A-1-1 | 1.500 | $5.55 \times 10^{-3}$ | 21.3 |
| (80%) | | | |
| A-1-3 | 1.125 | $2.50 \times 10^{-3}$ | 18.0 |
| (80%) | 1.312 | $3.75 \times 10^{-3}$ | 19.8 |
| | 2.000 | $1.38 \times 10^{-2}$ | 25.9 |
| A-3-3 | 1.125 | $1.25 \times 10^{-3}$ | 18.0 |
| (80%) | 1.312 | $2.34 \times 10^{-3}$ | 19.8 |
| | 1.812 | $1.00 \times 10^{-2}$ | 24.1 |

# APPENDIX C.

## SPECIMEN FABRICATION

The technique employed to fabricate the GRP plates from which specimens were to be cut was intended to approximate an actual production technique. The hand lay-up used no pressure or heat other than the manually-applied force of the men making the plates and the heat that developed from the exothermic curing process.

The chopped fiber, random mat glass ($1\frac{1}{2}$ oz/ft$^2$ - Stevens Fiberglass Co.) and the woven roving glass fabric (Style 779; 18 oz/yd$^2$; 9 strands per 2 inches warp, 7 strands per 2 inches fill - Stevens Fiberglass Co.) were cut from 38" wide rolls in sections 30" long and placed aside. A rigid wooden platform, 48" by 48", was covered with a sheet of mylar to prevent adhesion of the matrix to the wood. The amount of matrix required was determined largely by trial-and-error to be about 150% of the amount calculated to be necessary to provide a finished plate with a volume fraction of about 30%. The excess resin permitted work to progress at a quick enough pace so that the plate was not too far along in its cure before its completion.

The resin (number 4155 Laminac polyester resin - American Cyanamid Co.) was weighed in a five-gallon container. Methyl ethyl ketone peroxide (Specialty Chemicals Division; Reichold Chemicals, Inc.) was weighed in a separate container in an amount equal to 0.5% by weight of the resin and

then thoroughly mixed with the resin.

A generous amount of the activated resin was spread on the mylar-covered platform. A single layer of chopped mat was placed on the resin and more resin was poured over it. The resin was worked into the entire area of the glass mat using aluminum rollers. One layer of woven roving and one layer of random mat were then added and additional resin was worked into the entire area. The final six layers of glass were added in three steps in the same manner. The resin was always applied on the random mat to avoid spreading the strands of the woven roving when working the resin into the glass cloth. Firm pressure on the rollers insured adequate penetration of the resin and complete wetting of the glass fibers.

Another sheet of mylar was then placed on top of the uncured plate and steel shims, 0.185" thick, were laid parallel to all four sides. A steel pipe was placed across the plate and rested on the shims. Pressure was applied to the pipe by two men while rolling it across the plate to force out air and excess resin. The shims served to control plate thickness to achieve the desired volume fraction. The plate was then allowed to cure overnight and was removed the next day for eventual marking, cutting and machining.

Completed plates were marked and numbered for specimen preparation as shown in Figures 1a-c. The specimen layout provided 3/16" over final dimensions to allow for cutting

error and machining. A table saw with an installed dia-
mond-impregnated blade was used to cut the specimen shapes
from the plates. Final machining was accomplished using
a router installed inverted in a Tensil-Kut table.

The shape for the dogbone specimens was obtained using
a template developed experimentally and made by Kashihara
(5) for a separate study. The shape development was based
on photoelastic observations to eliminate stress concen-
trations. The final dogbone specimens were 10" long,
2" wide at the ends and were parallel-sided for a length of
$1\frac{1}{2}$" at the middle of the neck. Minimum width of the neck
was $1\frac{1}{2}$".

The index card specimens were drilled in a drill press
with a $\frac{1}{2}$" carbide-tipped bit. Notches $1\frac{1}{2}$" long were cut
using a 0.025" thick diamond-impregnated blade installed in
a shaper.

For all specimens, the weak direction of the woven
roving was parallel to the line of action of the applied
force. One consequence of the hand lay-up technique was
a moderate amount of variation in thickness from one loca-
tion to another within a plate. Thickness measurements
were taken of all specimens prior to testing and a global
average of all specimen thicknesses (74 specimens) was
used where required in the calculations. The global average
thickness was 0.216 inch.

# APPENDIX D.

## DESCRIPTION OF APPARATUS

The apparatus used to obtain the basic data consisted
of an Instron Model 1211 Dynamic Cycler, a circulating salt
water presoak bath, and a specially-designed salt water
containment system.  Supplementary data were obtained using
an Instron Universal Testing Machine and an Instron Univer-
sal Static/Dynamic Testing Instrument Model 1250.

All fatigue testing was performed on an Instron Model
1211 Dynamic Cycler which is a self-contained testing instru-
ment capable of automatically maintaining a preset fatigue
load cycle on an installed specimen.  The machine applies a
sinusoidal load cycle in either tension-only or tension-
compression.  The mean load must be preset but the operator
is free to choose the other parameter to control in the
load cycle.  When a notched specimen, in which a crack grows
over an interval of many cycles, is used or when the speci-
men is made of a material that undergoes significant plas-
tic deformation before complete failure, the load is held
constant by an increase in the stroke of the ram to which
the lower grip assembly is attached.  Control of the stroke
can be maintained manually or automatically.  The frequency
of load reversals can be controlled between 4 and 35 Hz.
Loads are read as percentages of full range with full load
ranges of 2,000, 4,000, and 10,000 pounds available.  Total
number of cycles applied to a specimen are displayed on a

frequency counter which advances one digit for every ten cycles.

It is a characteristic of this machine that an interval of about 100 cycles (at 6 Hz) is required for the machine to build up to the desired load cycle after the AUTO button is depressed. Similarly, when a specimen fractures, the machine stops itself by driving the ram to its lower limit but continues to count cycles during this process. These factors were probably responsible for some inaccuracies in the data although careful attention was paid at the beginning and end of testing each specimen. Figure 3 shows the build-up, running and drive-down portions of the load cycle. The machine is shown in Figures 4a - d and the gripping assemblies are shown in Figures 5a - b.

The circulating salt water presoak bath was used to soak specimens for ten-day periods prior to testing in salt water. It was comprised of a copper tank 30" long, 15" high and 15" wide and an electrically-driven pump. Specimens were placed in a wooden rack weighted down with granite slabs. The tank was filled with salt water to a depth sufficient to cover the specimens entirely. The motor-driven pump was used to circulate the water ( at room temperature) on an almost-continuous basis. The pump was stopped periodically to allow the motor to cool down. Salt water was added only to compensate for minor amounts lost through evaporation. (See Figure 6.)

In order to permit testing in a salt water environment,

a specially-designed salt water containment system was
built for installation on the Dynamic Cycler. The system
consisted of a box made of 3/8" plexiglas, open at the top
and holed at the bottom to accept the grip holder that
threaded into the ram of the Dynamic Cycler. Watertight-
ness was maintained at the hole by using a 1-3/4" rubber
O-ring and a 5" diameter custom-made retaining nut. Rigid,
watertight construction of the box was achieved by drilling
and tapping holes to accept 3/4", 10-24 zinc-plated screws.
All mating surfaces were coated with RTV silicone rubber
adhesive/sealant (General Electric Co.) prior to final
tightening of the screws. (See Figure 7.)

# APPENDIX E.

## K-CALIBRATION

The primary experimental K-calibration method used was that suggested by Irwin and Kies for the determination of strain energy release rate (7). Three index card specimens were chosen at random and were notched to a depth of one inch. Each specimen was pinned in an Instron Universal Testing Machine and loaded to about 200 pounds using a crosshead rate of 0.02 in/min and a chart speed of 2.0 in/min. The chart recorded load vs deflection between loading points. The notch length was then increased to one and one-eighth inch and the specimens were again loaded to 200 pounds. This procedure was continued with the notch length being increased by one-eighth inch between successive loadings until the notch length reached two and one-eighth inches at which time the notch increment was changed to one-fourth inch between loadings. When the notch length reached four and one-eighth inches, a crack began to grow at the end of the notch with the application of even the smallest load and no more data could be taken.

Using the chart records, the compliance of the specimen for each notch length was calculated as the inverse of the slope of the load-deflection curve;

$$C = \frac{\Delta l}{\Delta P} .$$

The values of C for the three specimens at each notch

length were then averaged and these values of $C_{ave}$ were plotted as a function of the notch length, a (measured from the center of the pin holes). The resulting curve was used to graphically determine values of $\frac{\partial C}{\partial a}$ as shown in Figure 9.

These values of $\frac{\partial C}{\partial a}$ were then plotted against notch length, a, and a smooth curve was drawn through the points. (See Figure 10.) For the remaining calculations, values of $\frac{\partial C}{\partial a}$ were taken from the curve rather than using the values obtained directly from the graphical technique.

Evaluation of strain energy release rate within each fatigue loading cycle was achieved by inserting the value of the maximum load in the cycle into the Irwin-Kies relationship;

$$G = \tfrac{1}{2} \, \frac{P_{max}^2}{B} \, \frac{\partial C}{\partial a} \, ,$$

where the values of $\frac{\partial C}{\partial a}$ were dictated by the observed values of crack length.

The stress intensity factor corresponding to each value of G was then found from;

$$K = \sqrt{GE} \, ,$$

where E was determined experimentally as described in Appendix F.

Data from the Irwin-Kies K-calibration are presented in Table 3. Data from the boundary collocation K-calibration are presented in Table 4.

# APPENDIX F.

## YOUNG'S MODULUS DETERMINATION

The value of Young's Modulus for the composite was
found experimentally from a simple tensile test.  Two
dogbone specimens, chosen at random, were each fitted
with two SR-4 strain gages (BLH Electronics), one to
measure longitudinal strain and the other to measure
transverse strain.  (Poisson's ratio for the material could
thus be determined although it was not used.)  The strain
gages were connected to a Wheatstone Bridge circuit which,
in turn, was connected to a Hewlitt-Packard 321 Dual
Channel Carrier Amplifier-Recorder.

The specimens were inserted into an Instron Universal
Testing Machine and loaded in tension to about 1800 pounds.
The load curve was recorded on the Instron recording chart
and the strain was recorded on the Hewlitt-Packard strip
recorder.  (The Hewlitt-Packard recorder actually gave an
output of $\frac{\Delta R}{R}$ in the bridge circuit.  Strain was computed
by dividing $\frac{\Delta R}{R}$ by the gage factor for the strain gage –
2.0 in this case.)  Stress was found by dividing load from
the Instron chart by the cross-sectional area of the test
piece at the location of the strain gage.

Young's Modulus for each of the two specimens was
measured and computed independently from the other using
Hooke's Law;

$$E = \frac{\sigma}{\varepsilon} .$$

The two values thus obtained were averaged to get a single value of E for use in the calculations to find K. The average value was found to be $E = 1.95 \times 10^3$ ksi.